



**HAL**  
open science

# A very easy high-order well-balanced reconstruction for hyperbolic systems with source terms

Christophe Berthon, Solène Bulteau, Françoise Foucher, Meissa M'Baye,  
Victor Michel-Dansac

## ► To cite this version:

Christophe Berthon, Solène Bulteau, Françoise Foucher, Meissa M'Baye, Victor Michel-Dansac. A very easy high-order well-balanced reconstruction for hyperbolic systems with source terms. 2021. hal-03271103v1

**HAL Id: hal-03271103**

**<https://hal.science/hal-03271103v1>**

Preprint submitted on 25 Jun 2021 (v1), last revised 4 Jul 2022 (v2)

**HAL** is a multi-disciplinary open access archive for the deposit and dissemination of scientific research documents, whether they are published or not. The documents may come from teaching and research institutions in France or abroad, or from public or private research centers.

L'archive ouverte pluridisciplinaire **HAL**, est destinée au dépôt et à la diffusion de documents scientifiques de niveau recherche, publiés ou non, émanant des établissements d'enseignement et de recherche français ou étrangers, des laboratoires publics ou privés.

1                    **A VERY EASY HIGH-ORDER WELL-BALANCED**  
2 **RECONSTRUCTION FOR HYPERBOLIC SYSTEMS WITH SOURCE**  
3 **TERMS\***

4    CHRISTOPHE BERTHON <sup>†</sup>, SOLÈNE BULTEAU <sup>‡</sup>, FRANÇOISE FOUCHER\*<sup>§</sup>, MEISSA  
5                    M'BAYE\*<sup>¶</sup>, AND VICTOR MICHEL-DANSAC <sup>||</sup>

6        **Abstract.** When adopting high-order finite-volume schemes based on MUSCL reconstruction  
7 techniques to approximate the weak solutions of hyperbolic systems with source terms, the preserva-  
8 tion of the steady states turns out to be very challenging. Indeed, the designed reconstruction must  
9 preserve the steady states under consideration in order to get the required well-balancedness prop-  
10 erty. A priori, to capture such a steady state, one needs to solve some strongly nonlinear equations.  
11 Here, in order to preserve the required well-balancedness property to be satisfied by finite volume  
12 methods, we design a very easy correction. This correction can be applied to any scheme of order  
13 greater than or equal to 2, such as a MUSCL-type scheme, and ensures that this scheme exactly  
14 preserves the steady solutions. The main discrepancy with usual techniques lies in never having to  
15 invert the nonlinear function governing the steady solutions. Moreover, for under-determined steady  
16 solutions, several nonlinear functions must be considered simultaneously. Since the derived correc-  
17 tion only considers the evaluation of the governing nonlinear functions, we are able to deal with  
18 under-determined stationary systems. Several numerical experiments illustrate the relevance of the  
19 proposed well-balanced correction.

20        **Key words.** Hyperbolic conservation laws, Balance laws, Well-balanced schemes, High-order  
21 reconstruction techniques

22        **AMS subject classifications.** 65M08, 65M12

23        **1. Introduction.**

24        **1.1. General framework.** The present work is devoted to the numerical ap-  
25 proximation of the weak solutions of an evolution law of the form

26 (1.1)                     $\partial_t w + \partial_x f(w) = S(w, x), \quad x \in \mathbb{R}, \quad t > 0,$

27 where  $w : \mathbb{R} \times \mathbb{R}^+ \rightarrow \Omega \subset \mathbb{R}^N$  denotes the unknown vector. The set  $\Omega$  stands for  
28 the set of the admissible states and it is assumed to be convex. The flux function  
29  $f : \Omega \rightarrow \mathbb{R}^n$  and the source term  $S : \Omega \times \mathbb{R} \rightarrow \mathbb{R}^N$  are assumed to be smooth enough,  
30 say  $C^1$ . For stability reasons, in the present work, the matrix  $\nabla_w f(w)$  is assumed  
31 to be diagonalizable in  $\mathbb{R}$  so that the homogeneous system extracted from (1.1) is  
32 hyperbolic. The PDE system (1.1) is endowed with initial data  $w(x, t = 0) = w^0(x)$ ,  
33 where  $w^0(x) \in \Omega$  for all  $x \in \mathbb{R}$  is a given function.

34        Because of the source term  $S(w, x)$ , there exists non-trivial steady solutions gov-

---

\*Submitted to the editors June 25, 2021.

**Funding:** C. Berthon acknowledges the support of ANR MUFFIN ANR-19-CE46-0004.

<sup>†</sup> Université de Nantes, CNRS UMR 6629, Laboratoire de Mathématiques Jean Leray, 2 rue de la Houssinière, BP 92208, 44322 Nantes, France ([Christophe.Berthon@univ-nantes.fr](mailto:Christophe.Berthon@univ-nantes.fr), <https://www.math.sciences.univ-nantes.fr/~berthon/WEBenglish/berthon.html>).

<sup>‡</sup> Maison de la Simulation, USR 3441, FR-91191 Gif-sur-Yvette ([solene.bulteau1@gmail.com](mailto:solene.bulteau1@gmail.com), <https://solenebulteau.wordpress.com>).

<sup>§</sup> École Centrale de Nantes, CNRS UMR 6629, Laboratoire de Mathématiques Jean Leray, 1 rue de La Noë, BP 92101, 44321 Nantes Cedex 3, France ([françoise.foucher@ec-nantes.fr](mailto:françoise.foucher@ec-nantes.fr)).

<sup>¶</sup> Laboratoire de Mathématiques de la Décision et d'Analyse Numérique (LMDAN), FASEG, Université Cheikh Anta Diop, BP 16889, Dakar, Sénégal ([meissaths@gmail.com](mailto:meissaths@gmail.com)).

<sup>||</sup> Université de Strasbourg, CNRS, Inria, IRMA, F-67000 Strasbourg, France ([victor.michel-dansac@inria.fr](mailto:victor.michel-dansac@inria.fr), [http://irma.math.unistra.fr/~micheldansac/index\\_en.html](http://irma.math.unistra.fr/~micheldansac/index_en.html)).

35 earned by

$$36 \quad (1.2) \quad \begin{cases} \partial_x f(w) = S(w, x), \\ w(x_0) = w_0, \end{cases}$$

37 where  $w_0$  is a given state in  $\Omega$  and  $x_0$  a given point in  $\mathbb{R}$ .

38 Now, if the above system can be integrated, there exists  $G : \Omega \times \mathbb{R} \rightarrow \mathbb{R}^N$  such  
39 that the stationary solutions are governed by

$$40 \quad \begin{cases} \partial_x G(w, x) = 0, \\ w(x_0) = w_0. \end{cases}$$

41 In fact, it is not always possible to integrate (1.2). Even then,  $G$  is not necessarily  
42 unique and, in general, it must be restricted according to some invariant domains.  
43 Usually, the steady solutions are restricted to some particular definition of  $G$ . Then,  
44 we have to deal with a sequence  $(G_\ell)_{1 \leq \ell \leq L}$  with  $L < +\infty$  given.

45 Equipped with these comments, in this work, we only consider steady solutions  
46 defined by

$$47 \quad (1.3) \quad \begin{cases} \partial_x G_\ell(w, x) = 0, & 1 \leq \ell \leq L, \\ w(x_0) = \Pi_\ell^{eq}(w_0), \end{cases}$$

48 where we have denoted by  $\Pi^{eq}(w)$  the projection of  $w$  over the invariant domain under  
49 consideration.

50 **1.2. Illustrating models.** In order to illustrate the relevance of such a defini-  
51 tion of the steady states, let us present some examples of particular interest. First,  
52 let us adopt the well-known shallow water model given by

$$53 \quad (1.4) \quad w = \begin{pmatrix} h \\ q \end{pmatrix}, \quad f(w) = \begin{pmatrix} q \\ \frac{q^2}{h} + g\frac{h^2}{2} \end{pmatrix}, \quad S(w, x) = \begin{pmatrix} 0 \\ -gh\partial_x z \end{pmatrix},$$

54 where  $g > 0$  is the gravity constant,  $z(x)$  the given smooth topography function,  $h$   
55 is the water height and  $q$  is the water discharge. The smooth steady solutions (see  
56 [4, 11, 25]) are given by

$$57 \quad (1.5) \quad \begin{cases} \partial_x q = 0, \\ \partial_x \left( \frac{q^2}{2h^2} + g(h+z) \right) = 0, \end{cases}$$

58 with  $w(x_0) = w_0$  for a given  $w_0$  in  $\Omega$ , where the set  $\Omega$  of admissible states is defined  
59 as follows:

$$60 \quad (1.6) \quad \Omega = \{ {}^t(h, q) \in \mathbb{R}^2; h \geq 0, q \in \mathbb{R} \}.$$

61 As a consequence, we immediately obtain

$$62 \quad (1.7) \quad G(w, x) = \begin{pmatrix} q \\ \frac{q^2}{2h^2} + g(h+z) \end{pmatrix} \quad \text{and} \quad \Pi^{eq}(w) = w.$$

63 Now, let us restrict the definition of the steady states just considering the usual  
64 lake at rest given by  $q = 0$  and  $\partial_x(h + z) = 0$ , then we easily get

$$65 \quad (1.8) \quad G(w, x) = \begin{pmatrix} 0 \\ h + z \end{pmatrix} \quad \text{and} \quad \Pi^{eq}(w) = \begin{pmatrix} h \\ 0 \end{pmatrix}.$$

66 The second example we present is given by the shallow water equations with a  
67 Manning friction source term (see [36, 34, 18]). This model reads

$$68 \quad (1.9) \quad w = \begin{pmatrix} h \\ q \end{pmatrix}, \quad f(w) = \begin{pmatrix} q \\ \frac{q^2}{h} + g\frac{h^2}{2} \end{pmatrix}, \quad S(w, x) = \begin{pmatrix} 0 \\ -\kappa \frac{q|q|}{h^\eta} \end{pmatrix},$$

69 where  $\kappa > 0$  is the friction coefficient and  $\eta \neq 1$  is the Manning exponent. The set of  
70 the admissible states is given by (1.6). After [36], the stationary solutions are given  
71 as follows:

$$72 \quad \begin{cases} \partial_x q = 0, \\ \partial_x \left( -q^2 \frac{h^{\eta-1}}{\eta-1} + g \frac{h^{\eta+2}}{\eta+2} + \kappa x q |q| \right) = 0, \end{cases}$$

73 with  $w(x_0) = w_0$  for a given  $w_0 \in \Omega$ , so that we immediately obtain

$$74 \quad (1.10) \quad G(w, x) = \begin{pmatrix} q \\ -q^2 \frac{h^{\eta-1}}{\eta-1} + g \frac{h^{\eta+2}}{\eta+2} + \kappa x q |q| \end{pmatrix} \quad \text{and} \quad \Pi^{eq}(w) = w.$$

75 Next, we present a system involving a non-unique definition of  $G$ , the Euler model  
76 with gravity (see [19, 45]). This model reads as follows:

$$77 \quad (1.11) \quad w = \begin{pmatrix} \rho \\ q \\ E \end{pmatrix}, \quad f(w) = \begin{pmatrix} q \\ \frac{q^2}{\rho} + p \\ (E + p) \frac{q}{\rho} \end{pmatrix}, \quad S(w, x) = \begin{pmatrix} 0 \\ -\rho \partial_x \varphi \\ -q \partial_x \varphi \end{pmatrix},$$

78 where  $\varphi : \mathbb{R} \rightarrow \mathbb{R}$  stands for a given smooth gravitational potential and  $p := p(\rho, E -$   
79  $\frac{1}{2} \frac{q^2}{\rho})$  denotes the pressure law, with  $E$  the total energy. The set of admissible states  
80 is defined here by

$$81 \quad \Omega = \left\{ t(\rho, q, E) \in \mathbb{R}^3; \rho > 0, q \in \mathbb{R}, E - \frac{1}{2} \frac{q^2}{\rho} > 0 \right\}.$$

82 Concerning the steady solutions, we are concerned by steady solutions at rest governed  
83 by (see [19, 45])

$$84 \quad \begin{cases} q = 0, \\ \partial_x p + \rho \partial_x \varphi = 0, \end{cases} \quad \text{with} \quad w(x_0) = \begin{pmatrix} \rho_0 \\ 0 \\ E_0 \end{pmatrix}.$$

85 Once again, the system to govern the steady state solutions turns out to be under-  
86 determined and we have to focus on particular families of steady solutions. According

87 to [19, 45], three families of steady states are of prime importance. The first family  
88 is given by

$$89 \quad \begin{cases} q = 0, \\ \partial_x \rho = 0, \\ \partial_x (p + \rho \varphi) = 0, \end{cases} \quad \text{with} \quad w(x_0) = \begin{pmatrix} \rho_0 \\ 0 \\ E_0 \end{pmatrix},$$

90 for all  $\rho_0 > 0$  and  $E_0 > 0$ .

91 In order to define both second and third families of steady states, we have to  
92 impose that the function  $E \mapsto p(\rho, E)$  is invertible and we denote by  $p_E^{-1}(\rho, \cdot)$  this  
93 inverse function so that  $p_E^{-1}(\rho, p(\rho, E)) = E$ . Now, the second steady state family  
94 reads

$$95 \quad \begin{cases} q = 0, \\ \partial_x (p - \kappa \rho) = 0, \\ \partial_x (\varphi + \kappa \ln \rho) = 0, \end{cases} \quad \text{with} \quad w(x_0) = \begin{pmatrix} \rho_0 \\ 0 \\ p_E^{-1}(\rho_0, \kappa \rho_0) \end{pmatrix},$$

96 where  $\kappa > 0$  is a given parameter. The last steady state family is defined by

$$97 \quad (1.12) \quad \begin{cases} q = 0, \\ \partial_x (p - \kappa \rho^\gamma) = 0, \\ \partial_x \left( \frac{\kappa \gamma}{\gamma - 1} \rho^{\gamma-1} + \varphi \right) = 0, \end{cases} \quad \text{with} \quad w(x_0) = \begin{pmatrix} \rho_0 \\ 0 \\ p_E^{-1}(\rho_0, \kappa \rho_0^\gamma) \end{pmatrix},$$

98 where  $\gamma > 1$  is a given parameter.

99 As a consequence, we get

(1.13)

$$100 \quad G_1(w, x) = \begin{pmatrix} q \\ \rho \\ p + \rho \varphi \end{pmatrix}, \quad G_2(w, x) = \begin{pmatrix} q \\ p - \kappa \rho \\ \varphi + \kappa \ln \rho \end{pmatrix}, \quad G_3(w, x) = \begin{pmatrix} q \\ p - \kappa \rho^\gamma \\ \frac{\kappa \gamma}{\gamma - 1} \rho^{\gamma-1} + \varphi \end{pmatrix},$$

101 with

(1.14)

$$102 \quad \Pi_1^{eq}(w) = \begin{pmatrix} \rho \\ 0 \\ E \end{pmatrix}, \quad \Pi_2^{eq}(w) = \begin{pmatrix} \rho \\ 0 \\ p_E^{-1}(\rho, \kappa \rho) \end{pmatrix} \quad \text{and} \quad \Pi_3^{eq}(w) = \begin{pmatrix} \rho \\ 0 \\ p_E^{-1}(\rho, \kappa \rho^\gamma) \end{pmatrix}.$$

103 **1.3. Main motivations.** Now, considering the derivation of numerical schemes  
104 approximating the solutions of (1.1) and able to accurately, or even exactly, capture  
105 the steady solutions defined by (1.3) has been an important challenge during the two  
106 last decades. Numerous techniques have been designed for the shallow water model  
107 with topography (1.4) supplemented by the lake at rest (1.8). For a non-exhaustive  
108 bibliography, the reader is referred to [2, 11, 4, 9, 32, 38, 22, 16, 13, 17, 8]. More  
109 recently, in [5, 6, 36, 35, 37, 42, 44, 25], extensions are given in order to deal with  
110 moving steady states given by (1.7). In [36, 28, 12], the Manning-type friction source  
111 term is adopted and suitable discretizations are introduced to capture steady states  
112 given by (1.10). Regarding the discretization of the Euler model with gravity (1.11),  
113 the reader is referred to [19, 3, 14, 29, 31, 33, 43, 45, 15] where numerical strategies

114 are developed to capture steady states according to the pairs  $(G_\ell, \Pi_\ell^{eq})$  defined by  
 115 (1.13) – (1.14).

116 In the present work, we are not interested in the derivation of well-balanced  
 117 schemes, namely schemes able to capture steady solutions given by (1.3). Here, our  
 118 purpose concerns the high-order extensions obtained by involving a polynomial re-  
 119 construction procedure. Indeed, as soon as the well-balancedness property must be  
 120 preserved, the reconstruction may involve strong difficulties. In particular, to be well-  
 121 balanced, the usual reconstruction approaches need to invert  $G_\ell(w, x)$  with respect  
 122 to  $w$  for one given  $\ell$  as long as the function  $w \mapsto G_\ell(w, x)$  is invertible. We im-  
 123 mediately understand that dealing simultaneously with distinct functions  $G_\ell(w, x)$   
 124 does not seem reachable. Moreover, imposing that the application  $w \mapsto G_\ell(w, x)$  is  
 125 invertible is a strong assumption, not satisfied in general by physical models.

126 In this work, we present a very easy strategy to force any reconstruction proce-  
 127 dure to preserve the steady solutions given by (1.3) just evaluating the applications  
 128  $G_\ell(w, x)$  according to the projection  $\Pi_\ell^{eq}(w)$ . To address such an issue, the present  
 129 work is organized as follows. In order to set the framework and the main notations,  
 130 in section 2 we introduce the numerical schemes and the usual MUSCL second-order  
 131 strategy [41, 30, 40]. In addition, we present the main issues when enforcing the poly-  
 132 nomial reconstruction to be well-balanced. Section 3 is then devoted to the strategy  
 133 designed here, which ensures that the expected well-balancedness property is satisfied  
 134 by any reconstruction. The proposed improvement comes from a suitable evaluation  
 135 of the pairs  $(G_\ell, \Pi_\ell^{eq})_{1 \leq \ell \leq L}$ ;  $G_\ell$  is never inverted. In section 4, we present a high-order  
 136 well-balanced extension. To conclude the paper, section 5 is devoted to several numer-  
 137 ical experiments to illustrate the relevance of the designed high-order reconstruction  
 138 improvement.

139 **2. Issues of the well-balanced second-order MUSCL schemes.** To ap-  
 140 proximate the solutions of (1.1), the space is discretized by introducing a sequence  
 141 of cells  $(x_{i-\frac{1}{2}}, x_{i+\frac{1}{2}})$ , for all  $i \in \mathbb{Z}$ , with a constant size  $\Delta x$ . We denote by  $x_i =$   
 142  $(x_{i-\frac{1}{2}} + x_{i+\frac{1}{2}})/2$  the center of each cell. We set  $t^{n+1} = t^n + \Delta t$  to discretize the  
 143 time domain with a time step  $\Delta t$ . In general,  $\Delta t$  is restricted according to a CFL  
 144 condition.

145 At time  $t^n$ , we denote by  $w_i^n$  a constant approximation of the solution of (1.1)  
 146 over the cell  $(x_{i-\frac{1}{2}}, x_{i+\frac{1}{2}})$ . To evolve this approximation in time, we adopt a finite  
 147 volume scheme of the form

$$148 \quad (2.1) \quad w_i^{n+1} = w_i^n - \frac{\Delta t}{\Delta x} \left( f_{i+\frac{1}{2}}^n - f_{i-\frac{1}{2}}^n \right) + \frac{\Delta x}{2} \left( S_{i-\frac{1}{2}}^n + S_{i+\frac{1}{2}}^n \right),$$

149 where we have set

$$150 \quad f_{i+\frac{1}{2}}^n = f_\Delta(w_i^n, w_{i+1}^n) \quad \text{and} \quad S_{i+\frac{1}{2}}^n = S_\Delta(w_i^n, w_{i+1}^n, x_i, x_{i+1}, \Delta x).$$

151 In order to get a consistent scheme, the numerical flux function  $f_\Delta$  and the discrete  
 152 source term  $S_\Delta$  are assumed to be Lipschitz-continuous and to verify

$$153 \quad (2.2) \quad f_\Delta(w, w) = f(w) \quad \text{and} \quad S_\Delta(w, w, x, x, 0) = S(w, x).$$

154 At this level, the reader is referred to the large literature devoted to the derivation  
 155 of a well-balanced scheme according to the system of interest. Here, we have imposed  
 156 the well-balancedness property according to the definition (1.3) of the steady states.  
 157 As a consequence, we get  $w_i^{n+1} = w_i^n$  as long as, for all  $i$  in  $\mathbb{Z}$ , we have

$$158 \quad (2.3) \quad G_\ell(w_i^n, x_i) = G_\ell(w_{i+1}^n, x_{i+1}) \quad \text{and} \quad w_i^n = \Pi_\ell^{eq}(w_i^n) \quad \text{with} \quad 1 \leq \ell \leq L.$$

159 Now, we focus on a second-order extension, see for instance [40, 41, 7]. To address  
 160 such an issue, we have to introduce suitable reconstructed states, denoted by  $w_{i+\frac{1}{2}}^\pm$ ,  
 161 on each side of the interface  $x_{i+\frac{1}{2}}$ . This reconstruction is said to be second-order  
 162 accurate in space if, for all  $i \in \mathbb{Z}$ , we have

$$163 \quad (2.4) \quad w_{i+\frac{1}{2}}^- = w(x_{i+\frac{1}{2}}, t^n) + \mathcal{O}(\Delta x^2) \quad \text{and} \quad w_{i+\frac{1}{2}}^+ = w(x_{i+\frac{1}{2}}, t^n) + \mathcal{O}(\Delta x^2),$$

164 for some smooth function  $x \mapsto w(x, t^n)$  such that  $w_i^n = \frac{1}{\Delta x} \int_{x_{i-\frac{1}{2}}}^{x_{i+\frac{1}{2}}} w(x, t^n) dx$ .

165 Equipped with this second-order reconstruction, from the first-order scheme (2.1),  
 166 we define a second-order scheme as follows:

$$167 \quad (2.5) \quad w_i^{n+1} = w_i^n - \frac{\Delta t}{\Delta x} \left( f_{i+\frac{1}{2}}^\pm - f_{i-\frac{1}{2}}^\pm \right) + \Delta t S_i^\pm,$$

168 where we have set  $f_{i+\frac{1}{2}}^\pm = f_\Delta(w_{i+\frac{1}{2}}^-, w_{i+\frac{1}{2}}^+)$ , and where  $S_i^\pm$  is a second-order approxi-  
 169 mation of the source term average, i.e.

$$170 \quad (2.6) \quad S_i^\pm = \frac{1}{\Delta x} \int_{x_{i-\frac{1}{2}}}^{x_{i+\frac{1}{2}}} S(w(x, t^n), x) dx + \mathcal{O}(\Delta x^2).$$

171 A classical choice for such second-order accurate schemes is to use the second-order  
 172 midpoint approximation:

$$173 \quad (2.7) \quad S_i^\pm = S \left( \frac{1}{2} \left( w_{i-\frac{1}{2}}^+ + w_{i+\frac{1}{2}}^- \right), x_i \right).$$

174 It is clear that second-order accuracy is achieved as soon as the reconstructed  
 175 states are defined. At the interface  $x_{i+\frac{1}{2}}$ , the reconstructed states read (for instance,  
 176 see [7, 40, 41])

$$177 \quad (2.8) \quad \begin{aligned} w_{i+\frac{1}{2}}^- &= w_i^n + \frac{1}{2} \mathcal{L}(w_i^n - w_{i-1}^n, w_{i+1}^n - w_i^n), \\ w_{i+\frac{1}{2}}^+ &= w_{i+1}^n - \frac{1}{2} \mathcal{L}(w_{i+1}^n - w_i^n, w_{i+2}^n - w_{i+1}^n), \end{aligned}$$

178 where  $\mathcal{L} : \mathbb{R}^N \times \mathbb{R}^N \rightarrow \mathbb{R}^N$  are Lipschitz-continuous functions, which satisfy

$$179 \quad \mathcal{L}(w, w) = w \quad \text{for all } w \in \mathbb{R}^N,$$

$$180 \quad \exists M > 0 \text{ such that } \|\mathcal{L}(w_L, w_R)\| \leq M \max(\|w_L\|, \|w_R\|), \quad \forall w_L, w_R \in \mathbb{R}^N.$$

182 A large body of literature is devoted to introduce suitable definition of  $\mathcal{L}$  (for instance,  
 183 see [30] and references therein).

184 Now, by adopting (2.8), the steady states are, in general, not preserved by such a  
 185 reconstruction. Indeed, in order to recover the expected well-balancedness property,  
 186 we require

$$187 \quad (2.9) \quad w_{i+\frac{1}{2}}^- = w_i^n \quad \text{and} \quad w_{i+\frac{1}{2}}^+ = w_{i+1}^n \quad \text{for all } i \in \mathbb{Z},$$

188 as soon as  $(w_i^n)_{i \in \mathbb{Z}}$  defines a steady state according to (2.3). Except for linear steady  
 189 states, the steady condition (2.9) is lost. As a consequence, a particular attention  
 190 must be paid on the definition of  $\mathcal{L}$  to preserves the steady states.

191 Currently, the reconstruction on  $G_\ell$  instead of  $w$  is preferred (see [2, 24]). For a  
 192 fixed  $\ell$ , denoted by  $\ell^*$ , we perform the reconstruction as follows:

$$\begin{aligned}
 G_{i+\frac{1}{2}}^- &= G_{\ell^*}(w_i^n, x_i) \\
 &+ \frac{1}{2}\mathcal{L}\left(G_{\ell^*}(w_i^n, x_i) - G_{\ell^*}(w_{i-1}^n, x_{i-1}), G_{\ell^*}(w_{i+1}^n, x_{i+1}) - G_{\ell^*}(w_i^n, x_i)\right), \\
 193 \quad G_{i+\frac{1}{2}}^+ &= G_{\ell^*}(w_{i+1}^n, x_{i+1}) \\
 &- \frac{1}{2}\mathcal{L}\left(G_{\ell^*}(w_{i+1}^n, x_{i+1}) - G_{\ell^*}(w_i^n, x_i), G_{\ell^*}(w_{i+2}^n, x_{i+2}) - G_{\ell^*}(w_{i+1}^n, x_{i+1})\right),
 \end{aligned}$$

194 The reconstructed states  $w_{i+\frac{1}{2}}^\pm$  at the interface  $x_{i+\frac{1}{2}}$  are then defined by

$$195 \quad (2.10) \quad \begin{cases} G_{\ell^*}(w_{i+\frac{1}{2}}^-, x_{i+\frac{1}{2}}) = G_{i+\frac{1}{2}}^-, \\ G_{\ell^*}(w_{i+\frac{1}{2}}^+, x_{i+\frac{1}{2}}) = G_{i+\frac{1}{2}}^+. \end{cases}$$

196 We immediately remark that (2.9) holds as soon as  $(w_i^n)_{i \in \mathbb{Z}}$  defines a steady state  
 197 for  $G_{\ell^*}$  according to (2.3). However, the function  $w \mapsto G_{\ell^*}(w, x)$  must be inverted.  
 198 Such a procedure may be very costly, or even impossible to carry out if  $G_{\ell^*}(\cdot, x)$  is  
 199 not invertible.

200 In fact, in the simpler situation of the lake at rest for the shallow water equation,  
 201 where  $G$  is given by (1.8), we have to solve a linear  $2 \times 2$  system. But for a moving  
 202 steady state, i.e. with  $G$  defined by (1.7), the uniqueness of the reconstructed states  
 203  $w_{i+\frac{1}{2}}^\pm$  is no longer ensured. Next, considering (1.10), neither the existence nor the  
 204 uniqueness of  $w_{i+\frac{1}{2}}^\pm$  is ensured.

205 Moreover, adopting such a procedure needs to fix  $\ell$ . As a consequence, it is  
 206 not possible to deal with steady states governed by several families  $G_\ell(w, x)$  with  
 207  $1 \leq \ell \leq L$  for  $L \geq 2$ . Such a restriction arises for instance for the Euler equations  
 208 with gravity, where we consider three steady state families.

209 To summarize the failure of the usual well-balanced reconstruction technique, the  
 210 reconstructed states, solution of (2.10), may not exist or not be unique. Moreover,  
 211 since we have to solve a nonlinear system, the evaluation of the reconstructed states  
 212 turns out to be computationally expensive. In addition, such a reconstruction tech-  
 213 nique preserves only one steady state family while some systems involve several steady  
 214 state families.

215 **3. A very easy well-balanced MUSCL reconstruction.** The objective is  
 216 now to derive a reconstruction technique able to preserve the steady states but never  
 217 involving an inversion of  $G_\ell$ . To address such an issue, we suggest to improve the  
 218 usual reconstruction (2.8) as follows:

$$\begin{aligned}
 219 \quad (3.1) \quad \tilde{w}_{i+\frac{1}{2}}^- &= w_i^n + \frac{1}{2}\theta_{i+\frac{1}{2}}^n \mathcal{L}(w_i^n - w_{i-1}^n, w_{i+1}^n - w_i^n), \\
 \tilde{w}_{i+\frac{1}{2}}^+ &= w_{i+1}^n - \frac{1}{2}\theta_{i+\frac{1}{2}}^n \mathcal{L}(w_{i+1}^n - w_i^n, w_{i+2}^n - w_{i+1}^n),
 \end{aligned}$$

220 where the correction  $\theta_{i+\frac{1}{2}}^n$  must be an approximation of 1 at least with second-order  
 221 of accuracy which vanishes for pairs  $(w_i^n, w_{i+1}^n)$  satisfying (2.3). We propose the



222 following formulation of  $\theta_{i+\frac{1}{2}}^n$ :

$$223 \quad (3.2) \quad \theta_{i+\frac{1}{2}}^n = \frac{\varepsilon_{i+\frac{1}{2}}^n}{\varepsilon_{i+\frac{1}{2}}^n + \left(\frac{\Delta x}{C_{i+\frac{1}{2}}^n}\right)^k}, \text{ with}$$

$$224 \quad (3.3) \quad \varepsilon_{i+\frac{1}{2}}^n = \prod_{\ell=1}^L \left( \|G_\ell(w_{i+1}^n, x_{i+1}) - G_\ell(w_i^n, x_i)\| \right. \\ 225 \quad \left. + \|w_{i+1}^n - \Pi_\ell^{eq}(w_{i+1}^n)\| + \|w_i^n - \Pi_\ell^{eq}(w_i^n)\| \right),$$

226 where  $k \geq 2$  must be selected and where  $C_{i+\frac{1}{2}}^n \neq 0$  is any expression independent from  
227  $\Delta x$ . We shall suggest an expression of  $C_{i+\frac{1}{2}}^n$  in the numerical experiments. From now  
228 on, it is worth noting that  $\varepsilon_{i+\frac{1}{2}}^n = 0$  if and only if the pair  $(w_i^n, w_{i+1}^n)$  defines a local  
229 steady state, according to (2.3), at the interface  $x_{i+\frac{1}{2}}$ .

230 Concerning the source term discretization, we adopt the following definition:

$$231 \quad (3.4) \quad \tilde{S}_i^\pm = \frac{1}{2} \left( \left(1 - \theta_{i-\frac{1}{2}}^n\right) S_{i-\frac{1}{2}}^n + \left(1 - \theta_{i+\frac{1}{2}}^n\right) S_{i+\frac{1}{2}}^n \right) + \frac{1}{2} \left( \theta_{i-\frac{1}{2}}^n + \theta_{i+\frac{1}{2}}^n \right) S_i^\pm,$$

232 where  $S_i^\pm$  is given by (2.7) and where  $S_{i\pm\frac{1}{2}}^n$  comes from the first-order discretiza-  
233 tion (2.1). As a consequence, the second-order MUSCL scheme now reads

$$234 \quad (3.5) \quad w_i^{n+1} = w_i^n - \frac{\Delta t}{\Delta x} \left( f_{i+\frac{1}{2}}^\pm - f_{i-\frac{1}{2}}^\pm \right) + \Delta t \tilde{S}_i^\pm,$$

235 where we have set

$$236 \quad (3.6) \quad f_{i+\frac{1}{2}}^\pm = f_\Delta(\tilde{w}_{i+\frac{1}{2}}^-, \tilde{w}_{i+\frac{1}{2}}^+).$$

237 Before we establish the main properties satisfied by the second-order MUSCL  
238 scheme (3.5) – (3.6) with the reconstructed states (3.1) and the source term dis-  
239 cretization (3.4), let us recall the definition of the order of accuracy that is adopted  
240 here (for instance, see [11]).

241 DEFINITION 3.1. *For some smooth solution  $w(x, t)$  of (1.1), let us consider*

$$242 \quad (3.7) \quad w_i^n = \frac{1}{\Delta x} \int_{x_{i-\frac{1}{2}}}^{x_{i+\frac{1}{2}}} w(x, t^n) dx.$$

243 Define  $w_i^{n+1}$  by (2.5). The scheme (2.5) is said of order  $\tau$  in time and  $\delta$  in space if,  
244 for all  $i$  in  $\mathbb{Z}$ , we have

$$245 \quad (3.8) \quad w_i^{n+1} = \frac{1}{\Delta x} \int_{x_{i-\frac{1}{2}}}^{x_{i+\frac{1}{2}}} w(x, t^n + \Delta t) dx - \frac{\Delta t}{\Delta x} \left( \mathcal{F}_{i+\frac{1}{2}} - \mathcal{F}_{i-\frac{1}{2}} \right) + \Delta t \mathcal{S}_i,$$

246 where  $\mathcal{F}_{i+\frac{1}{2}} = \mathcal{O}(\Delta t^\tau) + \mathcal{O}(\Delta x^\delta)$  and  $\mathcal{S}_i = \mathcal{O}(\Delta t^\tau) + \mathcal{O}(\Delta x^\delta)$ .

247 Now, arguing the above definition of the order of accuracy, the improved reconstruc-  
248 tion technique based on  $\theta_{i+\frac{1}{2}}$  is established to yield a second-order accurate and  
249 well-balanced scheme.

250 THEOREM 3.2. *The scheme (3.5) – (3.6), with reconstructed states given by (3.1)*  
 251 *and a source term discretization given by (3.4), satisfies the following properties:*

- 252 (i) *it is second-order accurate in space for unsteady solutions;*  
 253 (ii) *it is well-balanced, i.e. it exactly preserves steady solutions: if  $(w_i^n)_{i \in \mathbb{Z}}$  defines*  
 254 *a steady state according to (2.3), then  $w_i^{n+1} = w_i^n$  for all  $i$  in  $\mathbb{Z}$ ;*  
 255 (iii) *it is robust, i.e. if the original reconstruction (2.8) preserves  $\Omega$ , then  $\Omega$  re-*  
 256 *mains invariant by the improved reconstruction (3.1).*

257 *Proof.* We establish properties (i), (ii) and (iii) in order.

- 258 (i) To establish the order of accuracy, let us consider  $w(x, t)$  a smooth unsteady  
 259 solution of (1.1). By integration of (1.1) over  $(x_{i-\frac{1}{2}}, x_{i+\frac{1}{2}}) \times (t^n, t^n + \Delta t)$ ,  
 260 we get

$$(3.9) \quad \begin{aligned} & \frac{1}{\Delta x} \int_{x_{i-\frac{1}{2}}}^{x_{i+\frac{1}{2}}} w(x, t^n + \Delta t) dx - \frac{1}{\Delta x} \int_{x_{i-\frac{1}{2}}}^{x_{i+\frac{1}{2}}} w(x, t^n) dx \\ & + \frac{\Delta t}{\Delta x} \left( \frac{1}{\Delta t} \int_{t^n}^{t^n + \Delta t} f(w(x_{i+\frac{1}{2}}, t)) dt - \frac{1}{\Delta t} \int_{t^n}^{t^n + \Delta t} f(w(x_{i-\frac{1}{2}}, t)) dt \right) \\ & = \Delta t \frac{1}{\Delta t \Delta x} \int_{t^n}^{t^n + \Delta t} \int_{x_{i-\frac{1}{2}}}^{x_{i+\frac{1}{2}}} S(w(x, t), x) dx dt. \end{aligned}$$

262 With  $(w_i^n)_{i \in \mathbb{Z}}$  given by (3.7) and  $(w_i^{n+1})_{i \in \mathbb{Z}}$  given by (3.5) – (3.6), a straight-  
 263 forward computation gives the expected relation (3.8), where we have set

$$(3.10) \quad \begin{aligned} \mathcal{F}_{i+\frac{1}{2}} &= f_{i+\frac{1}{2}}^\pm - \frac{1}{\Delta t} \int_0^{\Delta t} f(w(x_{i+\frac{1}{2}}, t^n + t)) dt, \\ \mathcal{S}_i &= \tilde{S}_i^\pm - \frac{1}{\Delta t \Delta x} \int_0^{\Delta t} \int_{x_{i-\frac{1}{2}}}^{x_{i+\frac{1}{2}}} S(w(x, t^n + t), x) dx dt, \end{aligned}$$

267 where  $f_{i+\frac{1}{2}}^\pm$  and  $\tilde{S}_i^\pm$  are respectively given by (3.6) and (3.4).

268 We first treat the approximation of the flux function. By definition of  $\theta_{i+\frac{1}{2}}^n$ ,  
 269 given by (3.2), as long as  $\varepsilon_{i+\frac{1}{2}}^n$  does not vanish, we have  $\theta_{i+\frac{1}{2}}^n = 1 + \mathcal{O}(\Delta x^k)$ .  
 270 As a consequence, in the current unsteady context, we get

$$(3.11) \quad \tilde{w}_{i+\frac{1}{2}}^- = w_{i+\frac{1}{2}}^- + \mathcal{O}(\Delta x^k) \quad \text{and} \quad \tilde{w}_{i+\frac{1}{2}}^+ = w_{i+\frac{1}{2}}^+ + \mathcal{O}(\Delta x^k),$$

272 where  $w_{i+\frac{1}{2}}^\pm$  are given by (2.8), and with  $k \geq 2$ . Since (2.4) holds for the  
 273 second-order polynomial reconstruction, we immediately obtain

$$(3.12) \quad \tilde{w}_{i+\frac{1}{2}}^- = w(x_{i+\frac{1}{2}}, t^n) + \mathcal{O}(\Delta x^2) \quad \text{and} \quad \tilde{w}_{i+\frac{1}{2}}^+ = w(x_{i+\frac{1}{2}}, t^n) + \mathcal{O}(\Delta x^2).$$

275 Assuming a Lipschitz-continuous numerical flux function such that the consi-  
 276 stency condition (2.2) holds, we have

$$(3.13) \quad f_{i+\frac{1}{2}}^\pm = f(w(x_{i+\frac{1}{2}}, t^n)) + \mathcal{O}(\Delta x^2),$$

278 and we get  $\mathcal{F}_{i+\frac{1}{2}} = \mathcal{O}(\Delta t) + \mathcal{O}(\Delta x^2)$ .

279 Next, we study the accuracy of the source term discretization. By definition  
280 of the source term reconstruction (3.4), we have

$$281 \quad \tilde{S}_i^\pm = S_i^\pm + \mathcal{O}(\Delta x^2),$$

282 and arguing (2.6) immediately yields  $\mathcal{S}_i = \mathcal{O}(\Delta x^2) + \mathcal{O}(\Delta t)$ .

283 Arguing Definition 3.1, the second-order space accuracy is thus established.

284 (ii) Concerning the preservation of the steady states, as soon as  $(w_i^n)_{i \in \mathbb{Z}}$  sat-  
285 isfy (2.3), we easily get  $\varepsilon_{i+\frac{1}{2}}^n = 0$  for all  $i$  in  $\mathbb{Z}$ . As a consequence, we  
286 have  $\theta_{i+\frac{1}{2}}^n = 0$ , which leads to

$$287 \quad \tilde{w}_{i+\frac{1}{2}}^- = w_i^n \text{ and } \tilde{w}_{i+\frac{1}{2}}^+ = w_{i+1}^n,$$

288 while  $\tilde{S}_i^\pm = \frac{1}{2}(S_{i-\frac{1}{2}}^n + S_{i+\frac{1}{2}}^n)$ . Put in other words, the reconstruction vanishes  
289 for steady states. Then, the original well-balanced first-order scheme (2.1) is  
290 recovered and the steady states are preserved.

291 (iii) We finally turn to the robustness of the improved reconstructed states  $\tilde{w}_{i+\frac{1}{2}}^\pm$ .

292 We remark that

$$293 \quad \tilde{w}_{i+\frac{1}{2}}^- = (1 - \theta_{i+\frac{1}{2}}^n)w_i^n + \theta_{i+\frac{1}{2}}^n w_{i+\frac{1}{2}}^- \text{ and } \tilde{w}_{i+\frac{1}{2}}^+ = (1 - \theta_{i+\frac{1}{2}}^n)w_{i+1}^n + \theta_{i+\frac{1}{2}}^n w_{i+\frac{1}{2}}^+,$$

294 where  $\theta_{i+\frac{1}{2}}^n$ , defined by (3.2), belongs to  $[0, 1]$ , and where  $w_{i+\frac{1}{2}}^\pm$  are given by  
295 the initial reconstruction (2.8). Since the states  $w_i^n$ ,  $w_{i+1}^n$  and  $w_{i+\frac{1}{2}}^\pm$  belong to  
296  $\Omega$ , the states  $\tilde{w}_{i+\frac{1}{2}}^\pm$  turn out to be convex combinations of states in  $\Omega$ . With  
297  $\Omega$  a convex set, we immediately deduce that  $\tilde{w}_{i+\frac{1}{2}}^\pm$  are in  $\Omega$ .

298 The proof is thus completed.  $\square$

299 To conclude this section, we emphasize that we have designed a well-balanced  
300 reconstruction procedure by only evaluating  $(G_\ell(w_i^n, x_i))_{1 \leq \ell \leq L}$  and never solving some  
301 nonlinear equations. Moreover, the introduced procedure simultaneously deals with  
302 all the involved families of steady states and it is not necessary to give more importance  
303 to one than to another.

304 **4. Well-balanced high-order extension.** The above well-balanced improve-  
305 ment for the second-order MUSCL scheme is easily extended to yield a well-balanced  
306 and high-order accurate scheme. To address such an issue, let us first introduce a  
307 high-order reconstruction according to existing works, see for instance [20, 21]. With  
308  $w(x, t)$  a given smooth function, we define  $w_i^n$  by adopting (3.7). Now, we consider  
309 the following polynomial reconstruction of degree  $d$  in space:

$$310 \quad (4.1) \quad p_w^n(x; i) = w_i^n + \pi_i^w(x - x_i),$$

311 where  $\pi_i^w$  is a polynomial function of degree  $d$  such that, for all  $x \in (x_{i-\frac{1}{2}}, x_{i+\frac{1}{2}})$ , we  
312 have

$$313 \quad (4.2) \quad p_w^n(x; i) = w(x, t^n) + \mathcal{O}(\Delta x^{d+1}) \quad \text{and} \quad \frac{1}{\Delta x} \int_{x_{i-\frac{1}{2}}}^{x_{i+\frac{1}{2}}} p_w^n(x; i) dx = w_i^n.$$

314 Equipped with this reconstruction of degree  $d$ , a scheme of space order  $\delta = d + 1$  is  
315 derived. The reader is referred to [20, 21] where such reconstruction techniques are  
316 derived.

317 From this high-order reconstruction, we now give the associated high-order well-  
 318 balanced scheme to approximate the weak solutions of (1.1) as follows:

$$319 \quad (4.3) \quad w_i^{n+1} = w_i^n - \frac{\Delta t}{\Delta x} \left( f_{i+\frac{1}{2}}^\pm - f_{i-\frac{1}{2}}^\pm \right) + \Delta t \bar{S}_i^\pm,$$

320 with the numerical flux function given by (3.6), with

$$321 \quad (4.4) \quad w_{i+\frac{1}{2}}^- = (\tilde{p}_w^n)_i^+ \quad \text{and} \quad w_{i+\frac{1}{2}}^+ = (\tilde{p}_w^n)_{i+1}^-,$$

322 where  $(\tilde{p}_w^n)_i^\pm$  is the following well-balanced modification of the high-order polynomial  
 323 reconstruction (4.1) evaluated at the interface point  $x_{i\pm\frac{1}{2}}$ :

$$324 \quad (4.5) \quad (\tilde{p}_w^n)_i^\pm = w_i^n + \theta_{i\pm\frac{1}{2}}^n \pi_i^w \left( \pm \frac{\Delta x}{2} \right),$$

325 with  $\theta_{i\pm\frac{1}{2}}^n$  defined by (3.2) – (3.3). In (3.2), the parameter  $k$  must be fixed larger  
 326 than  $\delta = d + 1$  in order to preserve the order  $\delta$  of the polynomial reconstruction.  
 327 Concerning the source term approximation, we start with an approximation of order  $\delta$   
 328 of the source term average, as follows:

$$329 \quad (4.6) \quad S_i^\pm = \frac{1}{\Delta x} \int_{x_{i-\frac{1}{2}}}^{x_{i+\frac{1}{2}}} S(w(x, t^n), x) dx + \mathcal{O}(\Delta x^\delta).$$

330 In practice, this approximation is nothing but a quadrature formula of order  $\delta$ , see  
 331 for instance [1]. We then adopt the following well-balanced modification of this ap-  
 332 proximation:

$$333 \quad (4.7) \quad \bar{S}_i^\pm = \frac{1}{2} \left( (1 - \theta_{i-\frac{1}{2}}^n) S_{i-\frac{1}{2}}^n + (1 - \theta_{i+\frac{1}{2}}^n) S_{i+\frac{1}{2}}^n \right) + \frac{1}{2} \left( \theta_{i-\frac{1}{2}}^n + \theta_{i+\frac{1}{2}}^n \right) S_i^\pm.$$

334 At this level, it is worth noting that the  $\delta$ -order numerical scheme designed here  
 335 is obtained arguing a very easy modification (4.5) and (4.7) of any polynomial recon-  
 336 struction (4.1) of degree  $d$  and any source term integration (4.6) of order  $\delta$ . However,  
 337 this minor correction ensures that the scheme is well-balanced, is of order  $\delta$  in space,  
 338 and preserves the set of admissible states as soon as the original high-order scheme  
 339 does.

340 **THEOREM 4.1.** *The scheme (4.3), with the reconstructed states given by (4.4) and*  
 341 *the source term approximation (4.7), satisfies the following properties:*

- 342 (i) *it is of order  $\delta = d + 1$  in space for unsteady solutions;*
- 343 (ii) *it is well-balanced, i.e. it exactly preserves steady solutions:  $w_i^{n+1} = w_i^n$  for*  
 344 *all  $i \in \mathbb{Z}$  if  $(w_i^n)_{i \in \mathbb{Z}}$  define a steady state according to (2.3);*
- 345 (iii) *it is robust, i.e. if the original reconstruction (4.1) of degree  $d$  preserves  $\Omega$ ,*  
 346 *then  $\Omega$  remains invariant by the well-balanced improvement of the reconstruc-*  
 347 *tion (4.5).*

348 *Proof.* We establish properties (i), (ii) and (iii) in order.

- 349 (i) We first establish the order of accuracy, as defined in Definition 3.1. To ad-  
 350 dress such an issue, we consider  $w(x, t)$  a smooth unsteady solution of (1.1) so  
 351 that the relation (3.9) holds. Next, with  $(w_i^n)_{i \in \mathbb{Z}}$  given by (3.7) and  $(w_i^{n+1})_{i \in \mathbb{Z}}$

352 given by the high-order scheme (4.3), the relation (3.8) holds for

$$353 \quad \mathcal{F}_{i+\frac{1}{2}} = f_{i+\frac{1}{2}}^\pm - \frac{1}{\Delta t} \int_0^{\Delta t} f(w(x_{i+\frac{1}{2}}, t^n + t)) dt,$$

$$354 \quad \mathcal{S}_i = \bar{S}_i^\pm - \frac{1}{\Delta t \Delta x} \int_0^{\Delta t} \int_{x_{i-\frac{1}{2}}}^{x_{i+\frac{1}{2}}} S(w(x, t^n + t), x) dx dt,$$

355 where  $\bar{S}_i^\pm$  is defined by (4.7) and  $f_{i+\frac{1}{2}}^\pm$  by (3.6), with the high-order recon-  
357 structed states  $w_{i+\frac{1}{2}}^\pm$  given by (4.4).

358 Next, we establish the order of accuracy associated with the numerical flux  
359 function. First, because of the definition (3.2) of  $\theta_{i+\frac{1}{2}}^n$ , as long as  $\varepsilon_{i+\frac{1}{2}}^n$  does  
360 not vanish, a Taylor expansion yields

$$361 \quad \theta_{i+\frac{1}{2}}^n = 1 + \mathcal{O}(\Delta x^k), \quad \text{with } k \geq \delta = d + 1.$$

362 As a consequence, in the current unsteady context, by definition of the poly-  
363 nomial reconstruction according to (4.2), we obtain

$$364 \quad w_{i+\frac{1}{2}}^\pm = w(x_{i+\frac{1}{2}}, t^n) + \mathcal{O}(\Delta x^\delta).$$

365 Next, from (2.2), we know that the numerical flux function is Lipschitz-  
366 continuous and consistent. Therefore,

$$367 \quad f_\Delta(w_{i+\frac{1}{2}}^-, w_{i+\frac{1}{2}}^+) = f(w(x_{i+\frac{1}{2}}, t^n)) + \mathcal{O}(\Delta x^\delta),$$

368 and we get  $\mathcal{F}_{i+\frac{1}{2}} = \mathcal{O}(\Delta t) + \mathcal{O}(\Delta x^\delta)$ .

369 Concerning the order of accuracy of the source term, since (4.7) reduces to  
370  $\bar{S}_i^\pm = S_i^\pm + \mathcal{O}(\Delta x^\delta)$ , arguing (4.6) yields

$$371 \quad (4.8) \quad \bar{S}_i^\pm = \frac{1}{\Delta x} \int_{x_{i-\frac{1}{2}}}^{x_{i+\frac{1}{2}}} S(w(x, t^n), x) dx + \mathcal{O}(\Delta x^\delta).$$

372 Plugging (4.8) into the definition of  $\mathcal{S}_i$ , we get  $\mathcal{S}_i = \mathcal{O}(\Delta t) + \mathcal{O}(\Delta x^\delta)$ .

373 The establishment of the order of accuracy is thus completed.

- 374 (ii) For the proof of the well-balancedness property, let us consider  $(w_i^n)_{i \in \mathbb{Z}}$  to  
375 define a steady state according to (2.3). By definition of the correction,  
376 given by (3.2) – (3.3), we easily obtain  $\theta_{i+\frac{1}{2}}^n = 0$  for all  $i$  in  $\mathbb{Z}$  so that the  
377 reconstructed states now read

$$378 \quad w_{i+\frac{1}{2}}^- = w_i^n \text{ and } w_{i+\frac{1}{2}}^+ = w_{i+1}^n.$$

379 Similarly, regarding the source term reconstruction given by (4.7), we now  
380 have  $\bar{S}_i^\pm = \frac{1}{2}(S_{i-\frac{1}{2}}^n + S_{i+\frac{1}{2}}^n)$ . As a consequence, the high-order scheme (4.3)  
381 coincides with the first-order well-balanced scheme (2.1), and the preservation  
382 of the steady states immediately follows.

- 383 (iii) To conclude the proof, we now establish that the improvement (4.5) preserves  
384 the convex set  $\Omega$  as long as the original polynomial reconstruction (4.1) pre-  
385 serves  $\Omega$ . Indeed, we have

$$386 \quad (\tilde{p}_w^n)_i^\pm = \left(1 - \theta_{i\pm\frac{1}{2}}^n\right) w_i^n + \theta_{i\pm\frac{1}{2}}^n p_w^n \left(x \pm \frac{\Delta x}{2}; i\right).$$

387 Since  $p_w^n(x; i) \in \Omega$  for all  $x \in (x_{i-\frac{1}{2}}, x_{i+\frac{1}{2}})$ ,  $w_i^n \in \Omega$  and  $\theta_i^n \in [0, 1]$ , we  
 388 immediately get  $(\tilde{p}_w^n)_i^\pm \in \Omega$ .  
 389 The proof is thus completed.  $\square$

390 **5. Numerical experiments.** To assess the performance of the scheme devel-  
 391 oped above, we now perform several numerical experiments. First, we describe in  
 392 [subsection 5.1](#) the setup used to assess both the order of accuracy and the well-  
 393 balancedness property of the schemes under consideration. Then, we apply the high-  
 394 order well-balanced strategy to several systems, namely the shallow water equations  
 395 with topography (1.4) in [subsection 5.2](#), the shallow water equations with friction  
 396 (1.9) in [subsection 5.3](#), and the Euler equations with gravity (1.11) in [subsection 5.4](#).

397 **5.1. Setup.** To justify the relevance of the procedure outlined in [Sections 3](#)  
 398 and [4](#), we wish to compare the results of a given first-order well-balanced scheme to  
 399 the ones produced by its second-order and high-order extensions, with and without  
 400 the well-balancedness correction. For the sake of simplicity, we introduce the following  
 401 notations:

- 402 • the  $\mathbb{P}_d$  scheme is the scheme of order  $d + 1$  without the well-balancedness  
 403 correction,
- 404 • the  $\mathbb{P}_d^{\text{WB}}$  scheme is the scheme of order  $d + 1$  with the well-balancedness  
 405 correction.

406 Note that the  $\mathbb{P}_0$  and  $\mathbb{P}_0^{\text{WB}}$  schemes are identical. Furthermore, note that forcing  
 407  $\theta = 1$  on the whole space-time domain in the  $\mathbb{P}_d^{\text{WB}}$  scheme is enough to yield the  $\mathbb{P}_d$   
 408 scheme. In this paper, we consider high-order schemes up to a third-order accurate  
 409  $\mathbb{P}_2$  scheme. This is enough to justify both the high-order accuracy and the steady  
 410 state preservation.

411 To use the  $\mathbb{P}_d$  scheme, we need to define three elements: the polynomial recon-  
 412 struction from (4.1), the approximation of the source term average from (4.6), and  
 413 the time integration. These elements are summarized in [Table 1](#).

TABLE 1

*Polynomial reconstruction from (4.1), source term average from (4.6), and time integrator for the  $\mathbb{P}_1$  and  $\mathbb{P}_2$  schemes.*

	polynomial reconstruction	source term average	time integration
$\mathbb{P}_1$ scheme	MUSCL [41]	midpoint method	SSPRK2 [26, 27]
$\mathbb{P}_2$ scheme	third-order [39]	Simpson’s method	SSPRK3 [26, 27]

414 Moreover, recall that the  $\mathbb{P}_d^{\text{WB}}$  scheme is defined up to the choice of  $C_{i+\frac{1}{2}}^n$  in the  
 415 definition (3.2) of  $\theta_{i+\frac{1}{2}}^n$ . Heuristically, a good choice uses the numerical time derivative  
 416 of the solution. Let us define, for  $n \geq 1$ ,

$$417 \quad C_{i+\frac{1}{2}}^n = C_\theta \frac{1}{2} \left( \frac{\|W_{i+1}^n\| - \|W_{i+1}^{n-1}\|}{\Delta t} + \frac{\|W_i^n\| - \|W_i^{n-1}\|}{\Delta t} \right),$$

418 with  $C_\theta$  a constant parameter, which can be interpreted as a normalization of the time  
 419 derivative. The choice of  $C_\theta$  depends on the numerical experiment under consideration  
 420 (unless otherwise mentioned, we take  $C_\theta = 1$ ). We also take  $C_{i+\frac{1}{2}}^0 = 1$ . Note that,

421 equipped with this definition of  $C_{i+\frac{1}{2}}^n$ , the expression (3.2) of  $\theta_{i+\frac{1}{2}}^n$  reads:

$$422 \quad \theta_{i+\frac{1}{2}}^n = \frac{\varepsilon_{i+\frac{1}{2}}^n (C_{i+\frac{1}{2}}^n)^k}{\varepsilon_{i+\frac{1}{2}}^n (C_{i+\frac{1}{2}}^n)^k + \left(\frac{\Delta x}{C_\theta}\right)^k}.$$

423 Therefore, we get  $\theta_{i+\frac{1}{2}}^n = 0$  if  $\varepsilon_{i+\frac{1}{2}}^n = 0$  or if  $C_{i+\frac{1}{2}}^n = 0$ . This is justified in each case,  
424 as follows.

- 425 • If  $\varepsilon_{i+\frac{1}{2}}^n = 0$ , then a steady solution of the equations has been reached, and the  
426 first-order well-balanced scheme should be used to ensure the preservation of  
427 this solution. Taking  $\theta_{i+\frac{1}{2}}^n = 0$  enables this behavior.
- 428 • If  $C_{i+\frac{1}{2}}^n = 0$ , then a local steady solution of the  $\mathbb{P}_d$  scheme has been reached.  
429 Regardless of whether  $\varepsilon_{i+\frac{1}{2}}^n = 0$ , we should get  $\theta_{i+\frac{1}{2}}^n = 0$  in this case, since a  
430 steady solution for the  $\mathbb{P}_d$  scheme will not, in general, be a steady solution for  
431 the equations. Setting  $\theta_{i+\frac{1}{2}}^n = 0$  for such cases perturbs the steady numerical  
432 solution and allows it to converge towards the real steady solution.

433 We shall perform two experiments for each system, in order to validate both the  
434 high-order accuracy and the well-balancedness property. These experiments are de-  
435 tailed below; system-specific parameters (such as the final physical time, for instance)  
436 will be given in the relevant sections.

437 In each experiment, the space domain is  $(0, 1)$  and the simulation is run until  
438 some final time  $t_{\text{end}}$ . Each experiment relies on the following compactly supported  
439  $\mathcal{C}^\infty$  bump function:

$$440 \quad \omega(x) = \begin{cases} \exp\left(1 - \frac{1}{1 - (4(x - 1/2))^2}\right) & \text{if } |x - 1/2| < 1/4, \\ 0 & \text{otherwise.} \end{cases}$$

441 In addition, all errors computed in the remainder of the text are  $L^2$  errors between  
442 the approximate solution and the exact or reference solution.

443 The first experiment we perform yields a measure of the order of accuracy of  
444 the schemes, and it is designed to show that the well-balancedness correction does  
445 not reduce the accuracy for unsteady solutions. To correctly measure the order of  
446 accuracy, no slope limitation is added to the  $\mathbb{P}_d$  and  $\mathbb{P}_d^{\text{WB}}$  schemes. Since we do not  
447 necessarily know an exact solution of the system under consideration, we compute a  
448 reference solution using a very fine grid made of  $20 \times 2^{12}$  cells. Then, after computing  
449 the approximate solution on a coarser dyadic grid made of  $N = 20 \times 2^k$  cells,  $0 \leq k <$   
450  $12$ , the fine solution is projected onto the coarser grid to measure the error between  
451 the reference solution and its approximation. To ensure that no shock waves form,  
452 the initial condition is smooth; its expression is given for each system. The initial  
453 condition is then evolved until the final time  $t_{\text{end}} = 5 \cdot 10^{-3}$ . Periodic boundary  
454 conditions are prescribed for this experiment.

455 The second experiment assesses the well-balancedness property. To that end, we  
456 study the dissipation of a perturbation applied to an initially steady solution. Here,  
457 we add a slope limitation to the  $\mathbb{P}_d$  and  $\mathbb{P}_d^{\text{WB}}$  schemes, namely the MC limiter from [30]  
458 for  $d = 1$  and the limiter from [39] for  $d = 2$ . The initial condition is a steady solution  
459  $W$ , computed by solving the nonlinear system (1.3). This steady solution is then  
460 perturbed using the bump function  $\omega$ . Namely, each variable in  $W$  is multiplied by  
461  $(1 + \omega(x)/4)$ . The steady solution is imposed on the boundaries, and the experiment

462 is run until the numerical solution becomes steady; this final time is given for each  
 463 system. We take 50 discretization cells for this experiment.

464 **5.2. Application: the shallow water equations with topography.** The  
 465 first application concerns the shallow water equations with topography (1.4). The  
 466 first-order well-balanced scheme comes from [35, 10]. It contains a parameter  $C$ ,  
 467 set here to  $\infty$ , or rather to the upper bound of the double-precision floating-point  
 468 numbers in practice. In addition, the topography function is set to  $Z(x) = \omega(x)$  and  
 469 we take  $g = 9.81$ .

470 **5.2.1. Order of accuracy assessment.** For this experiment, the initial condi-  
 471 tion is given by  $h_0(x) = 2 - Z(x) + \cos^2(2\pi x)$  and  $q_0(x) = \sin(2\pi x)$ .

472 In Figure 1, we display the reference solution and the approximations given by the  
 473  $\mathbb{P}_0$ ,  $\mathbb{P}_2$  and  $\mathbb{P}_2^{\text{WB}}$  schemes with 40 discretization cells. We observe that the third-order  
 474 schemes are very close to the reference solution, even with such a few cells.

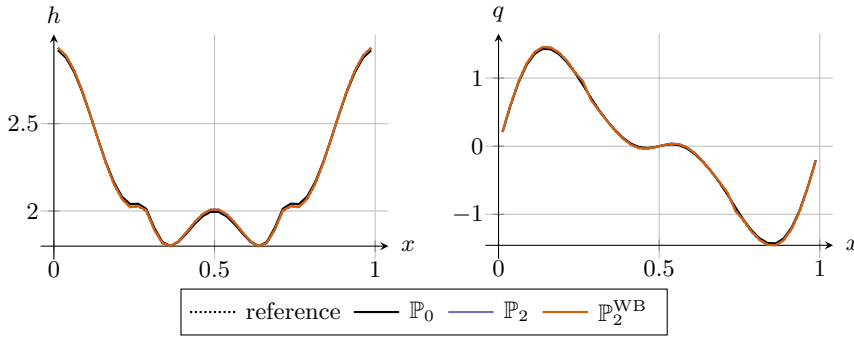


FIG. 1. Shallow water equations with topography: comparison between the reference and approximate solutions for the dyadic experiment with 40 discretization cells, at time  $t_{\text{end}} = 5 \cdot 10^{-3}$ . Left panel: water height  $h$ ; right panel: discharge  $q$ .

475 This observation is confirmed in Table 2 and Figure 2, where we report the errors  
 476 on  $h$  and  $q$ , as well as the orders of accuracy. As expected, the well-balancedness  
 477 procedure does not alter the order of accuracy of the scheme, since the solution pro-  
 478 duced by the  $\mathbb{P}_2^{\text{WB}}$  scheme is almost the same as the one produced by the  $\mathbb{P}_2$  scheme  
 479 in this unsteady context. We even observe a slight over-convergence, possibly ex-  
 480 plained by the use of the fourth-order accurate Simpson’s method in the source term  
 481 approximation.

482 **5.2.2. Well-balancedness property.** The initial condition is a perturbation of  
 483 the steady solution implicitly given by (1.5), with  $q = 1$  and  $\frac{q^2}{2h^2} + g(h + Z) = 2$ . We  
 484 take  $C_\theta = 9 \cdot 10^{-3}$ , and the final physical time is  $t_{\text{end}} = 20$ .

485 In Figure 3, we display the initial condition, as well as the approximations given  
 486 by the  $\mathbb{P}_0$ ,  $\mathbb{P}_2$  and  $\mathbb{P}_2^{\text{WB}}$  schemes at the time  $t = 2.5 \cdot 10^{-2}$ . We observe that the  
 487 solutions of the  $\mathbb{P}_2$  and  $\mathbb{P}_2^{\text{WB}}$  are quite close, even in this case of a perturbed steady  
 488 solution, and that they are less diffusive than the solution given by the  $\mathbb{P}_0$  scheme.

489 Then, in Figure 4 and Table 3, we report the errors on  $h$  and  $q$  at the final  
 490 time  $t_{\text{end}}$ . We observe that the  $\mathbb{P}_0$ ,  $\mathbb{P}_1^{\text{WB}}$  and  $\mathbb{P}_2^{\text{WB}}$  schemes have all converged towards  
 491 the exact steady solution up to machine precision, while a non-zero error remains for  
 492 the  $\mathbb{P}_1$  and  $\mathbb{P}_2$  schemes. These observations validate the proposed well-balancedness  
 493 correction.



TABLE 2

Shallow water equations with topography: errors and orders of accuracy for the dyadic experiment. For the sake of conciseness, only the errors on  $h$  are reported in this table; the reader is referred to Figure 2 for a visualization of the errors on  $q$ .

$N$	error, $\mathbb{P}_0$	order, $\mathbb{P}_0$	error, $\mathbb{P}_2$	order, $\mathbb{P}_2$	error, $\mathbb{P}_2^{\text{WB}}$	order, $\mathbb{P}_2^{\text{WB}}$
40	$1.04 \cdot 10^{-2}$	—	$1.12 \cdot 10^{-3}$	—	$1.12 \cdot 10^{-3}$	—
80	$5.24 \cdot 10^{-3}$	0.99	$3.25 \cdot 10^{-4}$	1.78	$3.26 \cdot 10^{-4}$	1.78
160	$2.58 \cdot 10^{-3}$	1.02	$4.06 \cdot 10^{-5}$	3.00	$4.08 \cdot 10^{-5}$	3.00
320	$1.29 \cdot 10^{-3}$	1.00	$2.74 \cdot 10^{-6}$	3.89	$2.73 \cdot 10^{-6}$	3.90
640	$6.42 \cdot 10^{-4}$	1.00	$1.76 \cdot 10^{-7}$	3.96	$1.76 \cdot 10^{-7}$	3.96
1280	$3.21 \cdot 10^{-4}$	1.00	$1.34 \cdot 10^{-8}$	3.72	$1.36 \cdot 10^{-8}$	3.69
2560	$1.60 \cdot 10^{-4}$	1.00	$1.50 \cdot 10^{-9}$	3.16	$1.54 \cdot 10^{-9}$	3.14

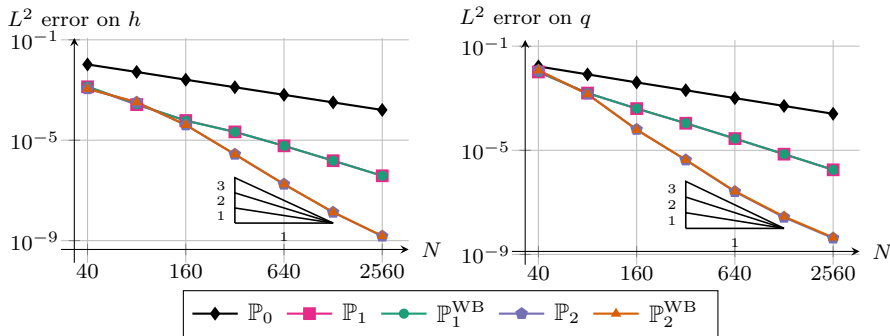


FIG. 2. Shallow water equations with topography: error lines for the dyadic experiment. Left panel: error on  $h$ ; right panel: error on  $q$ .

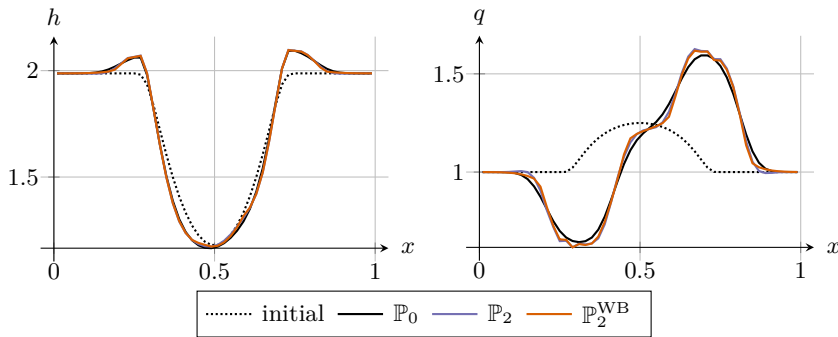


FIG. 3. Shallow water equations with topography: comparison between the initial condition and the approximate solutions at the time  $t = 2.5 \cdot 10^{-2}$ , for the perturbed steady state experiment with 50 cells. Left panel: water height  $h$ ; right panel: discharge  $q$ .

494 **5.3. Application: the shallow water equations with Manning friction.**

495 The next application concerns the shallow water equations with Manning friction,  
 496 governed by (1.9). The first-order well-balanced scheme comes from [36]. It also  
 497 contains a parameter  $C$ , also set here to  $\infty$ . We take the friction exponent  $\eta = 7/3$   
 498 according to Manning’s model [34, 18], and we set  $\kappa = 1$  as well as  $g = 9.81$ .

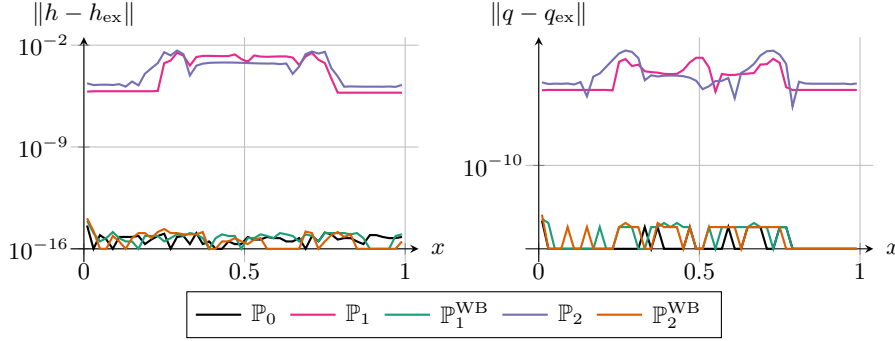


FIG. 4. Shallow water equations with topography: errors between the steady solution and the approximate solutions at the time  $t_{end}$ , for the perturbed steady state experiment with 50 cells. Left panel: error on  $h$ ; right panel: error on  $q$ .

TABLE 3

Shallow water equations with topography: errors between the steady solution and the approximate solutions at the time  $t_{end}$ , for the perturbed steady state experiment with 50 cells.

	error, $\mathbb{P}_0$	error, $\mathbb{P}_1$	error, $\mathbb{P}_1^{WB}$	error, $\mathbb{P}_2$	error, $\mathbb{P}_2^{WB}$
$h$	$7.55 \cdot 10^{-16}$	$1.22 \cdot 10^{-3}$	$1.40 \cdot 10^{-15}$	$1.30 \cdot 10^{-3}$	$1.92 \cdot 10^{-15}$
$q$	$2.15 \cdot 10^{-15}$	$1.67 \cdot 10^{-3}$	$3.62 \cdot 10^{-15}$	$5.43 \cdot 10^{-3}$	$4.87 \cdot 10^{-15}$

499 **5.3.1. Order of accuracy assessment.** The initial condition for this experi-  
 500 ment is given by  $h_0(x) = 2 + \cos^2(2\pi x)$  and  $q_0(x) = \sin(2\pi x)$ .  
 501 In Figure 5, we display the reference solution and the approximations given by  
 502 the  $\mathbb{P}_0$ ,  $\mathbb{P}_2$  and  $\mathbb{P}_2^{WB}$  schemes with 40 discretization cells. We once again observe that  
 503 the third-order schemes are very close to the reference solution.

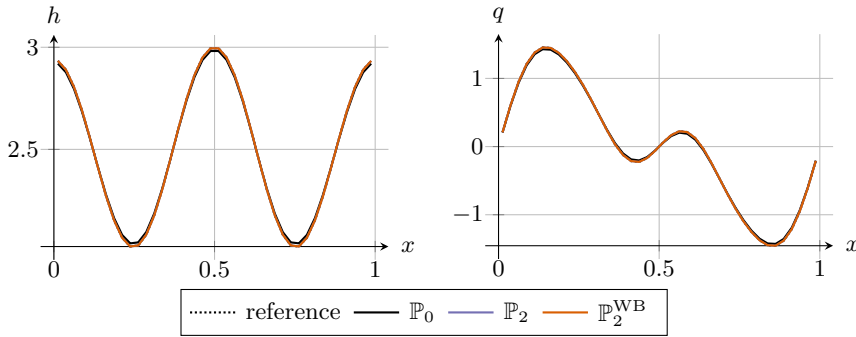


FIG. 5. Shallow water equations with Manning friction: comparison between the reference and approximate solutions for the dyadic experiment with 40 discretization cells, at time  $t_{end} = 5 \cdot 10^{-3}$ . Left panel: water height  $h$ ; right panel: discharge  $q$ .

504 We report the errors on  $h$  and  $q$ , as well as the orders of accuracy, in Table 4 and  
 505 Figure 6. The previous observation is once again confirmed since the  $\mathbb{P}_d$  and  $\mathbb{P}_d^{WB}$   
 506 schemes produce almost exactly the same solution for this experiment.

507 **5.3.2. Well-balancedness property.** The initial condition is a perturbation  
 508 of the steady solution implicitly given by (1.2), with  $q = 1$  and  $-q^2 \frac{h^{\eta-1}}{\eta-1} + g \frac{h^{\eta+2}}{\eta+2} +$

TABLE 4

Shallow water equations with Manning friction: errors and orders of accuracy for the dyadic experiment. For the sake of conciseness, only the errors on  $h$  are reported in this table; the reader is referred to [Figure 6](#) for a visualization of the errors on  $q$ .

$N$	error, $\mathbb{P}_0$	order, $\mathbb{P}_0$	error, $\mathbb{P}_2$	order, $\mathbb{P}_2$	error, $\mathbb{P}_2^{\text{WB}}$	order, $\mathbb{P}_2^{\text{WB}}$
40	$1.04 \cdot 10^{-2}$	—	$2.82 \cdot 10^{-4}$	—	$2.82 \cdot 10^{-4}$	—
80	$5.23 \cdot 10^{-3}$	1.00	$3.64 \cdot 10^{-5}$	2.95	$3.64 \cdot 10^{-5}$	2.95
160	$2.57 \cdot 10^{-3}$	1.03	$4.62 \cdot 10^{-6}$	2.98	$4.62 \cdot 10^{-6}$	2.98
320	$1.28 \cdot 10^{-3}$	1.00	$5.80 \cdot 10^{-7}$	2.99	$5.80 \cdot 10^{-7}$	2.99
640	$6.40 \cdot 10^{-4}$	1.00	$7.28 \cdot 10^{-8}$	3.00	$7.28 \cdot 10^{-8}$	3.00
1280	$3.20 \cdot 10^{-4}$	1.00	$9.11 \cdot 10^{-9}$	3.00	$9.11 \cdot 10^{-9}$	3.00
2560	$1.60 \cdot 10^{-4}$	1.00	$1.14 \cdot 10^{-9}$	3.00	$1.14 \cdot 10^{-9}$	3.00

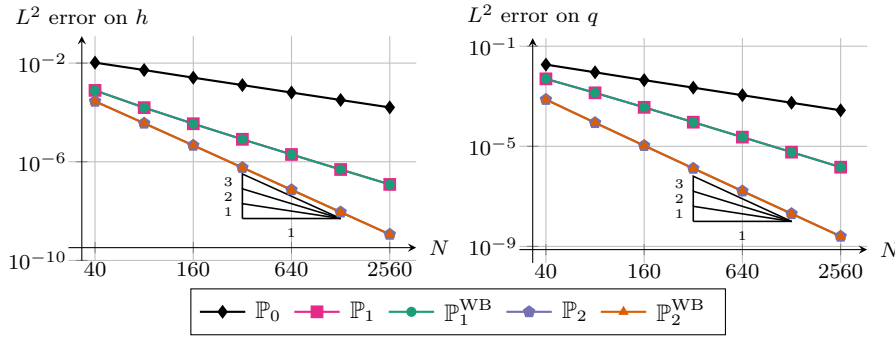


FIG. 6. Shallow water equations with Manning friction: error lines for the dyadic experiment. Left panel: error on  $h$ ; right panel: error on  $q$ .

509  $kq|q|x = 3$ . The final physical time is  $t_{\text{end}} = 20$ .

510 We display the initial condition, as well as the approximations produced by the  
 511  $\mathbb{P}_0$ ,  $\mathbb{P}_2$  and  $\mathbb{P}_2^{\text{WB}}$  schemes at the time  $t = 2.5 \cdot 10^{-2}$ , in [Figure 7](#). We observe that  
 512 the solutions of the  $\mathbb{P}_2$  and  $\mathbb{P}_2^{\text{WB}}$  are indistinguishable, and that they are less diffusive  
 513 than the solution given by the  $\mathbb{P}_0$  scheme.

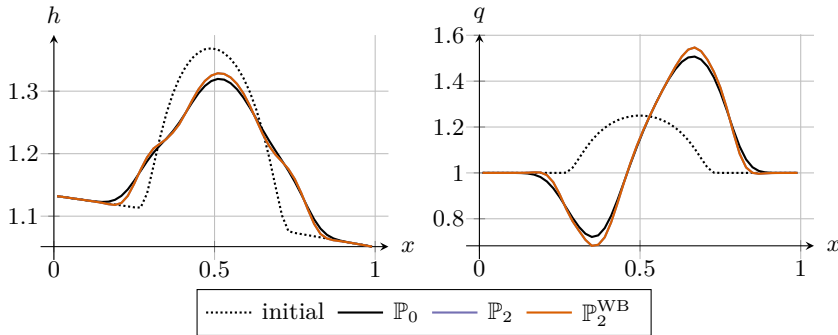


FIG. 7. Shallow water equations with Manning friction: comparison between the initial condition and the approximate solutions at the time  $t = 2.5 \cdot 10^{-2}$ , for the perturbed steady state experiment with 50 cells. Left panel: water height  $h$ ; right panel: discharge  $q$ .

514 In [Figure 8](#) and [Table 5](#), the errors on  $h$  and  $q$  at the final time  $t_{\text{end}}$  are reported.

515 Once again, the  $\mathbb{P}_0$ ,  $\mathbb{P}_1^{\text{WB}}$  and  $\mathbb{P}_2^{\text{WB}}$  schemes have all converged towards the exact  
 516 steady solution, and the  $\mathbb{P}_1$  and  $\mathbb{P}_2$  schemes produce a non-zero error.

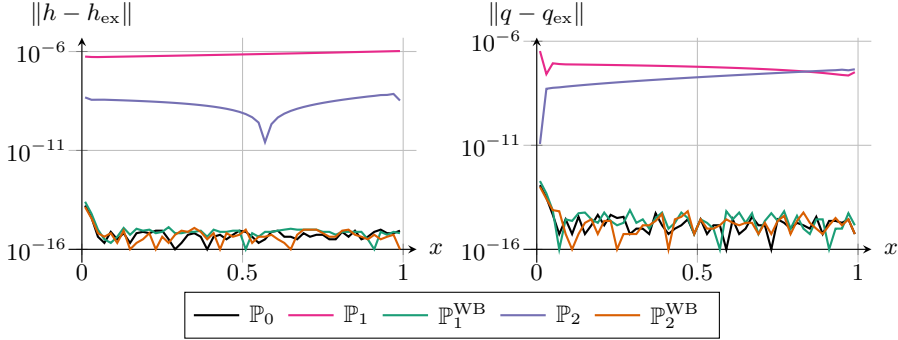


FIG. 8. Shallow water equations with Manning friction: errors between the steady solution and the approximate solutions at the time  $t_{\text{end}}$ , for the perturbed steady state experiment with 50 cells. Left panel: error on  $h$ ; right panel: error on  $q$ .

TABLE 5

Shallow water equations with Manning friction: errors between the steady solution and the approximate solutions at the time  $t_{\text{end}}$ , for the perturbed steady state experiment with 50 cells.

	error, $\mathbb{P}_0$	error, $\mathbb{P}_1$	error, $\mathbb{P}_1^{\text{WB}}$	error, $\mathbb{P}_2$	error, $\mathbb{P}_2^{\text{WB}}$
$h$	$2.43 \cdot 10^{-15}$	$7.63 \cdot 10^{-7}$	$3.79 \cdot 10^{-15}$	$3.24 \cdot 10^{-9}$	$2.08 \cdot 10^{-15}$
$q$	$1.79 \cdot 10^{-14}$	$7.53 \cdot 10^{-8}$	$2.84 \cdot 10^{-14}$	$2.40 \cdot 10^{-8}$	$1.51 \cdot 10^{-14}$

517 **5.4. Application: the Euler equations with gravity.** For the last applica-  
 518 tion, we turn to another system to highlight the genericness of our method. We choose  
 519 the Euler equations with gravity (1.11). The first-order well-balanced scheme is based  
 520 on the strategy from [35, 36, 23]. It is designed to exactly preserve and capture the  
 521 family of steady states given by (1.12). We consider an ideal gas pressure law, where  
 522 the pressure  $p$  is given by  $p = (\gamma - 1)(E - \frac{1}{2} \frac{q^2}{\rho})$ . Furthermore, we take the parameters  
 523  $\gamma = 1.4$  and  $\kappa = 1$ . The gravity potential is given by  $\varphi(x) = \omega(x)$ .

524 **5.4.1. Order of accuracy assessment.** For this experiment, we take the initial  
 525 condition  $\rho_0(x) = 2 + \cos^2(2\pi x)$ ,  $q_0(x) = \sin(2\pi x)$ ,  $E_0(x) = 5 + \cos^2(2\pi x)$ .

526 In Figure 9, we display the reference solution and the approximations given by  
 527 the  $\mathbb{P}_0$ ,  $\mathbb{P}_2$  and  $\mathbb{P}_2^{\text{WB}}$  schemes with 40 discretization cells. As usual, the third-order  
 528 schemes are very close to the reference solution.

529 We also report the errors and the orders of accuracy for  $\rho$ ,  $q$  and  $E$  in Table 6  
 530 and Figure 10. The same conclusion as for the shallow water system with topography  
 531 or Manning friction is drawn.

532 **5.4.2. Well-balancedness property.** The initial condition is a perturbation of  
 533 the steady solution implicitly given by (1.12), with  $q = 0$ ,  $p - \kappa\rho = 1$  and  $\kappa\gamma \frac{\rho^{\gamma-1}}{\gamma-1} + \varphi =$   
 534  $5$ . The final physical time is  $t_{\text{end}} = 300$ .

535 We display the initial condition, as well as the approximations produced by the  
 536  $\mathbb{P}_0$ ,  $\mathbb{P}_2$  and  $\mathbb{P}_2^{\text{WB}}$  schemes at the time  $t = 1 \cdot 10^{-1}$ , in Figure 11. The solutions of the

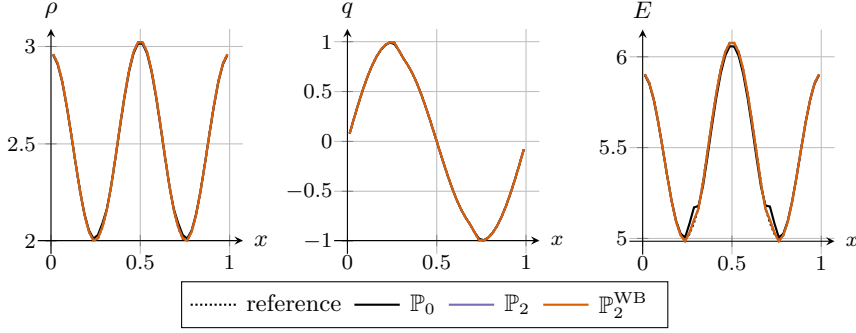


FIG. 9. Euler equations with gravity: comparison between the reference and approximate solutions for the dyadic experiment with 40 discretization cells, at time  $t_{end} = 5 \cdot 10^{-3}$ . Left panel: density  $\rho$ ; middle panel: momentum  $q$ ; right panel: energy  $E$ .

TABLE 6

Euler equations with gravity: errors and orders of accuracy for the dyadic experiment. For the sake of conciseness, only the errors on  $\rho$  are reported in this table; the reader is referred to Figure 6 for a visualization of the errors on  $q$  and  $E$ .

$N$	error, $\mathbb{P}_0$	order, $\mathbb{P}_0$	error, $\mathbb{P}_2$	order, $\mathbb{P}_2$	error, $\mathbb{P}_2^{WB}$	order, $\mathbb{P}_2^{WB}$
80	$4.18 \cdot 10^{-3}$	—	$2.61 \cdot 10^{-4}$	—	$2.61 \cdot 10^{-4}$	—
160	$2.07 \cdot 10^{-3}$	1.01	$5.59 \cdot 10^{-5}$	2.22	$5.59 \cdot 10^{-5}$	2.22
320	$1.03 \cdot 10^{-3}$	1.01	$1.09 \cdot 10^{-5}$	2.36	$1.09 \cdot 10^{-5}$	2.36
640	$5.14 \cdot 10^{-4}$	1.00	$1.72 \cdot 10^{-6}$	2.66	$1.72 \cdot 10^{-6}$	2.66
1280	$2.56 \cdot 10^{-4}$	1.00	$2.31 \cdot 10^{-7}$	2.89	$2.31 \cdot 10^{-7}$	2.89
2560	$1.28 \cdot 10^{-4}$	1.00	$2.95 \cdot 10^{-8}$	2.97	$2.95 \cdot 10^{-8}$	2.97
5120	$6.41 \cdot 10^{-5}$	1.00	$3.70 \cdot 10^{-9}$	2.99	$3.70 \cdot 10^{-9}$	2.99

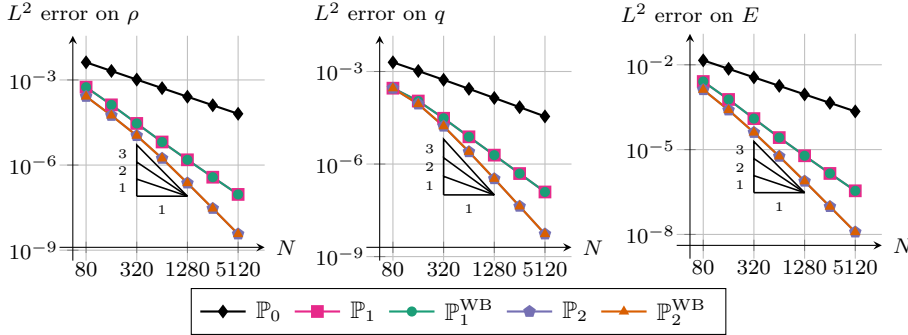


FIG. 10. Euler equations with gravity: error lines for the dyadic experiment. Left panel: error on  $\rho$ ; middle panel: error on  $q$ ; right panel: error on  $E$ .

537  $\mathbb{P}_2$  and  $\mathbb{P}_2^{WB}$  are once again indistinguishable and less diffusive than the one given by  
 538 the  $\mathbb{P}_0$  scheme.

539 In Figure 12 and Table 7, the errors on  $\rho$ ,  $q$  and  $E$  at the final time  $t_{end}$  are  
 540 reported. The same conclusions as in the shallow water case are reached.

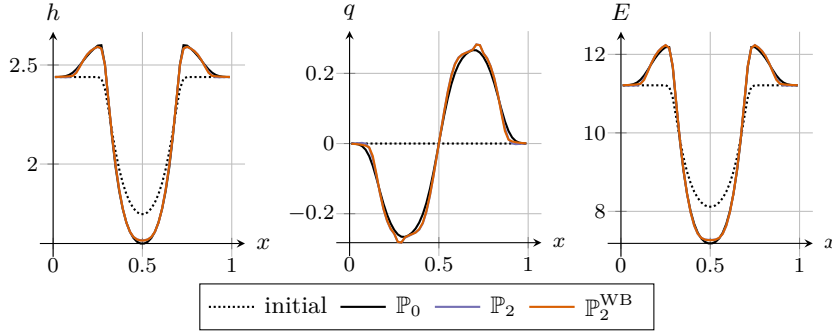


FIG. 11. Euler equations with gravity: comparison between the initial condition and the approximate solutions at the time  $t = 1 \cdot 10^{-1}$ , for the perturbed steady state experiment with 50 cells. Left panel: density  $\rho$ ; middle panel: momentum  $q$ ; right panel: energy  $E$ .

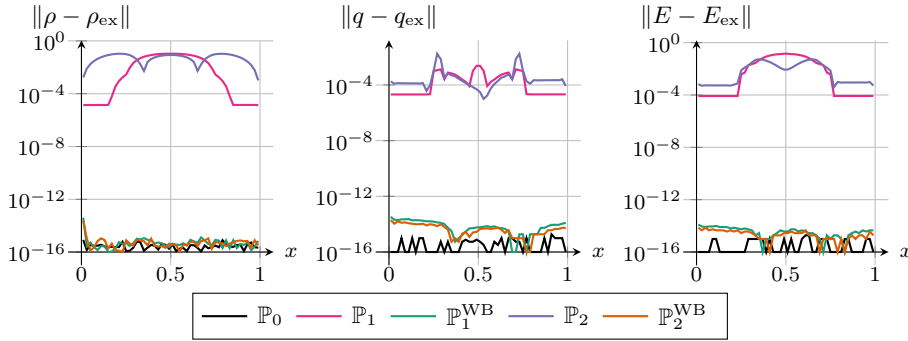


FIG. 12. Euler equations with gravity: errors between the steady solution and the approximate solutions at the time  $t_{end}$ , for the perturbed steady state experiment with 50 cells. Left panel: error on  $\rho$ ; middle panel: error on  $q$ ; right panel: error on  $E$ .

TABLE 7

Euler equations with gravity: errors between the steady solution and the approximate solutions at the time  $t_{end}$ , for the perturbed steady state experiment with 50 cells.

	error, $\mathbb{P}_0$	error, $\mathbb{P}_1$	error, $\mathbb{P}_1^{WB}$	error, $\mathbb{P}_2$	error, $\mathbb{P}_2^{WB}$
$\rho$	$2.64 \cdot 10^{-16}$	$5.44 \cdot 10^{-2}$	$5.75 \cdot 10^{-15}$	$6.77 \cdot 10^{-2}$	$3.42 \cdot 10^{-15}$
$q$	$5.60 \cdot 10^{-16}$	$7.14 \cdot 10^{-4}$	$1.20 \cdot 10^{-14}$	$3.83 \cdot 10^{-3}$	$7.01 \cdot 10^{-15}$
$E$	$6.47 \cdot 10^{-16}$	$6.19 \cdot 10^{-2}$	$5.12 \cdot 10^{-15}$	$2.31 \cdot 10^{-2}$	$3.05 \cdot 10^{-15}$

542 [1] M. ABRAMOWITZ AND I. A. STEGUN, eds., *Handbook of mathematical functions with formulas,*  
 543 *graphs, and mathematical tables*, Dover Publications, Inc., New York, 1992, <https://doi.org/10.2307/1266136>. Reprint of the 1972 edition.  
 544  
 545 [2] E. AUDUSSE, F. BOUCHUT, M.-O. BRISTEAU, R. KLEIN, AND B. PERTHAME, *A fast and*  
 546 *stable well-balanced scheme with hydrostatic reconstruction for shallow water flows*,  
 547 *SIAM J. Sci. Comput.*, 25 (2004), pp. 2050–2065, [http://epubs.siam.org/doi/abs/10.1137/](http://epubs.siam.org/doi/abs/10.1137/S1064827503431090)  
 548 [S1064827503431090](http://epubs.siam.org/doi/abs/10.1137/S1064827503431090).  
 549 [3] J. P. BERBERICH, P. CHANDRASHEKAR, C. KLINGENBERG, AND F. K. RÖPKE, *Second Order Fi-*  
 550 *nite Volume Scheme for Euler Equations with Gravity which is Well-Balanced for General*  
 551 *Equations of State and Grid Systems*, *Commun. Comput. Phys.*, 26 (2019), pp. 599–630,  
 552 <https://doi.org/10.4208/cicp.oa-2018-0152>.  
 553 [4] A. BERMUDEZ AND M. E. VAZQUEZ, *Upwind methods for hyperbolic conservation laws with*  
 554 *source terms*, *Comput. & Fluids*, 23 (1994), pp. 1049–1071, <http://www.sciencedirect.com>.

- 555 [com/science/article/pii/0045793094900043](https://doi.org/10.1007/s00574-016-0126-1).
- 556 [5] C. BERTHON AND C. CHALONS, *A fully well-balanced, positive and entropy-satisfying godunov-*  
557 *type method for the shallow-water equations*, Math. Comp., 85 (2016), pp. 1281–1307.
- 558 [6] C. BERTHON, C. CHALONS, S. CORNET, AND G. SPERONE, *Fully well-balanced, positive and*  
559 *simple approximate Riemann solver for shallow water equations*, Bull. Braz. Math. Soc.  
560 (N.S.), 47 (2016), pp. 117–130, <https://doi.org/10.1007/s00574-016-0126-1>, <http://dx.doi.org/10.1007/s00574-016-0126-1>.
- 561 [7] C. BERTHON AND V. DESVEAUX, *An entropy preserving MOOD scheme for the Euler equations*,  
562 Int. J. Finite Vol., 11 (2014).
- 563 [8] C. BERTHON AND F. FOUCHER, *Efficient well-balanced hydrostatic upwind schemes for shallow-*  
564 *water equations*, J. Comput. Phys., 231 (2012), pp. 4993–5015, <http://www.sciencedirect.com/science/article/pii/S0021999112001453>.
- 565 [9] C. BERTHON AND F. MARCHE, *A positive preserving high order VFRoe scheme for shallow water*  
566 *equations: a class of relaxation schemes*, SIAM J. Sci. Comput., 30 (2008), pp. 2587–2612,  
567 <https://doi.org/10.1137/070686147>, <http://dx.doi.org/10.1137/070686147>.
- 568 [10] C. BERTHON AND V. MICHEL-DANSAC, *A simple fully well-balanced and entropy preserv-*  
569 *ing scheme for the shallow-water equations*, Appl. Math. Lett., 86 (2018), pp. 284–290,  
570 <https://doi.org/10.1016/j.aml.2018.07.013>, [https://hal.archives-ouvertes.fr/hal-01708991/](https://hal.archives-ouvertes.fr/hal-01708991/document)  
571 [document](https://hal.archives-ouvertes.fr/hal-01708991/document).
- 572 [11] F. BOUCHUT, *Nonlinear stability of finite volume methods for hyperbolic conservation laws and*  
573 *well-balanced schemes for sources*, Frontiers in Mathematics, Birkhäuser Verlag, Basel,  
574 2004, <https://doi.org/10.1007/b93802>, <http://dx.doi.org/10.1007/b93802>.
- 575 [12] F. BOUCHUT, H. OUNAÏSSA, AND B. PERTHAME, *Upwinding of the source term at interfaces for*  
576 *Euler equations with high friction*, Comput. Math. Appl., 53 (2007), pp. 361–375.
- 577 [13] S. BRYSON, Y. EPSHTEYN, A. KURGANOV, AND G. PETROVA, *Well-balanced positivity preserv-*  
578 *ing central-upwind scheme on triangular grids for the Saint-Venant system*, ESAIM Math.  
579 Model. Numer. Anal., 45 (2011), pp. 423–446, <https://doi.org/10.1051/m2an/2010060>,  
580 <http://dx.doi.org/10.1051/m2an/2010060>.
- 581 [14] P. CARGO AND A.-Y. LE ROUX, *Un schéma équilibre adapté au modèle d’atmosphère avec*  
582 *termes de gravité*, C. R. Acad. Sci., Paris, Sér. I, 318 (1994), pp. 73–76, <http://cat.inist.fr/?aModele=afficheN&cpsidt=3409510>.
- 583 [15] C. CHALONS, F. COQUEL, E. GODLEWSKI, P.-A. RAVIART, AND N. SEGUIN, *Godunov-type*  
584 *schemes for hyperbolic systems with parameter-dependent source. The case of Euler sys-*  
585 *tem with friction*, Math. Models Methods Appl. Sci., 20 (2010), pp. 2109–2166, <https://doi.org/10.1142/S021820251000488X>,  
586 <http://dx.doi.org/10.1142/S021820251000488X>.
- 587 [16] G. CHEN AND S. NOELLE, *A new hydrostatic reconstruction scheme based on subcell recon-*  
588 *structions*, SIAM J. Numer. Anal., 55 (2017), pp. 758–784.
- 589 [17] Y. CHENG, A. CHERTOCK, M. HERTY, A. KURGANOV, AND T. WU, *A new approach for de-*  
590 *signing moving-water equilibria preserving schemes for the shallow water equations*, J. Sci.  
591 Comput., 80 (2019), pp. 538–554.
- 592 [18] O. DELESTRE, C. LUCAS, P.-A. KSNANT, F. DARBOUX, C. LAGUERRE, T.-N.-T. VO, F. JAMES,  
593 AND S. CORDIER, *SWASHES: a compilation of shallow water analytic solutions for hy-*  
594 *draulic and environmental studies*, Internat. J. Numer. Methods Fluids, 72 (2013), pp. 269–  
595 300, <https://doi.org/10.1002/flid.3741>.
- 596 [19] V. DESVEAUX, M. ZENK, C. BERTHON, AND C. KLINGENBERG, *A well-balanced scheme to cap-*  
597 *ture non-explicit steady states in the Euler equations with gravity*, Internat. J. Numer.  
598 Methods Fluids, 81 (2016), pp. 104–127.
- 599 [20] S. DIOT, S. CLAIN, AND R. LOUBÈRE, *Improved detection criteria for the multi-dimensional op-*  
600 *timal order detection (MOOD) on unstructured meshes with very high-order polynomials*,  
601 Comput. & Fluids, 64 (2012), pp. 43–63, <https://doi.org/10.1016/j.compfluid.2012.05.004>.
- 602 [21] S. DIOT, R. LOUBÈRE, AND S. CLAIN, *The multidimensional optimal order detection method in*  
603 *the three-dimensional case: very high-order finite volume method for hyperbolic systems*,  
604 Internat. J. Numer. Methods Fluids, 73 (2013), pp. 362–392, [https://doi.org/10.1002/flid.](https://doi.org/10.1002/flid.3804)  
605 [3804](https://doi.org/10.1002/flid.3804).
- 606 [22] J. M. GALLARDO, C. PARÉS, AND M. CASTRO, *On a well-balanced high-order finite vol-*  
607 *ume scheme for shallow water equations with topography and dry areas*, J. Com-  
608 put. Phys., 227 (2007), pp. 574–601, [http://www.sciencedirect.com/science/article/pii/](http://www.sciencedirect.com/science/article/pii/S0021999107003488)  
609 [S0021999107003488](http://www.sciencedirect.com/science/article/pii/S0021999107003488).
- 610 [23] B. GHITTI, C. BERTHON, M. H. LE, AND E. F. TORO, *A fully well-balanced scheme for the 1D*  
611 *blood flow equations with friction source term*, J. Comput. Phys., 421 (2020), p. 109750,  
612 <https://doi.org/10.1016/j.jcp.2020.109750>.
- 613 [24] I. GÓMEZ-BUENO, M. J. CASTRO, AND C. PARÉS, *High-order well-balanced methods for systems*

- of balance laws: a control-based approach, *Appl. Math. Comput.*, 394 (2021), p. 125820, <https://doi.org/10.1016/j.amc.2020.125820>.
- [25] L. GOSSE, *A well-balanced flux-vector splitting scheme designed for hyperbolic systems of conservation laws with source terms*, *Comput. Math. Appl.*, 39 (2000), pp. 135–159, [https://doi.org/10.1016/S0898-1221\(00\)00093-6](https://doi.org/10.1016/S0898-1221(00)00093-6).
- [26] S. GOTTLIEB AND C.-W. SHU, *Total variation diminishing Runge-Kutta schemes*, *Math. Comp.*, 67 (1998), pp. 73–85, <https://doi.org/10.1090/S0025-5718-98-00913-2>.
- [27] S. GOTTLIEB, C.-W. SHU, AND E. TADMOR, *Strong stability-preserving high-order time discretization methods*, *SIAM Rev.*, 43 (2001), pp. 89–112, <https://doi.org/10.1137/S003614450036757X>.
- [28] J.-L. GUERMOND, M. QUEZADA DE LUNA, B. POPOV, C. E. KEES, AND M. W. FARTHING, *Well-balanced second-order finite element approximation of the shallow water equations with friction*, *SIAM J. Sci. Comput.*, 40 (2018), pp. A3873–A3901.
- [29] R. KÄPPELI AND S. MISHRA, *Well-balanced schemes for the Euler equations with gravitation*, *J. Comput. Phys.*, 259 (2014), pp. 199 – 219, <https://doi.org/http://dx.doi.org/10.1016/j.jcp.2013.11.028>, <http://www.sciencedirect.com/science/article/pii/S0021999113007900>.
- [30] R. J. LEVEQUE, *Finite volume methods for hyperbolic problems*, *Cambridge Texts in Applied Mathematics*, Cambridge University Press, Cambridge, 2002, <https://doi.org/10.1017/CBO9780511791253>, <http://dx.doi.org/10.1017/CBO9780511791253>.
- [31] G. LI AND Y. XING, *Well-balanced discontinuous Galerkin methods with hydrostatic reconstruction for the Euler equations with gravitation*, *J. Comput. Phys.*, 352 (2018), pp. 445–462, <https://doi.org/10.1016/j.jcp.2017.09.063>, <https://doi.org/10.1016/j.jcp.2017.09.063>.
- [32] Q. LIANG AND F. MARCHE, *Numerical resolution of well-balanced shallow water equations with complex source terms*, *Adv. Water Resour.*, 32 (2009), pp. 873–884.
- [33] J. LUO, K. XU, AND N. LIU, *A well-balanced symplecticity-preserving gas-kinetic scheme for hydrodynamic equations under gravitational field*, *SIAM J. Sci. Comput.*, 33 (2011), pp. 2356–2381, <http://epubs.siam.org/doi/abs/10.1137/100803699>.
- [34] R. MANNING, *On the flow of water in open channels and pipes*, *Transactions of the Institution of Civil Engineers of Ireland*, 20 (1891), pp. 161–207.
- [35] V. MICHEL-DANSAC, C. BERTHON, S. CLAIN, AND F. FOUCHER, *A well-balanced scheme for the shallow-water equations with topography*, *Comput. Math. Appl.*, 72 (2016), pp. 568–593, <https://doi.org/10.1016/j.camwa.2016.05.015>, <https://hal.archives-ouvertes.fr/hal-01201825/document>.
- [36] V. MICHEL-DANSAC, C. BERTHON, S. CLAIN, AND F. FOUCHER, *A well-balanced scheme for the shallow-water equations with topography or Manning friction*, *J. Comput. Phys.*, 335 (2017), pp. 115–154.
- [37] S. NOELLE, Y. XING, AND C.-W. SHU, *High-order well-balanced finite volume WENO schemes for shallow water equation with moving water*, *J. Comput. Phys.*, 226 (2007), pp. 29–58, <https://doi.org/10.1016/j.jcp.2007.03.031>, <http://dx.doi.org/10.1016/j.jcp.2007.03.031>.
- [38] C. PARÉS AND M. CASTRO, *On the well-balance property of Roe’s method for nonconservative hyperbolic systems. Applications to shallow-water systems*, *M2AN Math. Model. Numer. Anal.*, 38 (2004), pp. 821–852, <https://doi.org/10.1051/m2an:2004041>, <http://dx.doi.org/10.1051/m2an:2004041>.
- [39] B. SCHMIDTMANN, B. SEIBOLD, AND M. TORRILHON, *Relations Between WENO3 and Third-Order Limiting in Finite Volume Methods*, *J. Sci. Comput.*, 68 (2015), pp. 624–652, <https://doi.org/10.1007/s10915-015-0151-z>.
- [40] E. F. TORO, *Riemann solvers and numerical methods for fluid dynamics*, Springer-Verlag, Berlin, third ed., 2009, <https://doi.org/10.1007/b79761>. A practical introduction.
- [41] B. VAN LEER, *Towards the ultimate conservative difference scheme. V. A second-order sequel to Godunov’s method*, *J. Comput. Phys.*, 32 (1979), pp. 101–136, <http://www.sciencedirect.com/science/article/pii/0021999179901451>.
- [42] Y. XING, *Exactly well-balanced discontinuous Galerkin methods for the shallow water equations with moving water equilibrium*, *J. Comput. Phys.*, 257 (2014), pp. 536–553, <https://doi.org/10.1016/j.jcp.2013.10.010>, <http://dx.doi.org/10.1016/j.jcp.2013.10.010>.
- [43] Y. XING AND C.-W. SHU, *High order well-balanced WENO scheme for the gas dynamics equations under gravitational fields*, *J. Sci. Comput.*, 54 (2013), pp. 645–662.
- [44] Y. XING, C.-W. SHU, AND S. NOELLE, *On the advantage of well-balanced schemes for moving-water equilibria of the shallow water equations*, *J. Sci. Comput.*, 48 (2011), pp. 339–349, <http://link.springer.com/article/10.1007/s10915-010-9377-y>.
- [45] K. XU, J. LUO, AND S. CHEN, *A well-balanced kinetic scheme for gas dynamic equations under gravitational field*, *Adv. Appl. Math. Mech.*, 2 (2010), pp. 200–210.